Geol. Mag. **141** (5), 2004, pp. 545–563. © 2004 Cambridge University Press
DOI: 10.1017/S0016756804009604 *Printed in the United Kingdom*

Cenozoic volcanism in the Middle East: petrogenesis of alkali basalts from northern Lebanon

ABDEL-FATTAH M. ABDEL-RAHMAN* & PHILIP E. NASSAR

Department of Geology, American University of Beirut, P.O. Box 11-0236, Beirut, Lebanon

(*Received* 9 December 2003; *accepted* 24 May 2004)

Abstract – The Cenozoic volcanic field of the Akkar region in northern Lebanon consists of a thick succession (200 m) of basaltic lava flows, erupted at the junction between a restraining bend (the Yammouneh transform fault) and its northern extension (the Ghab transform) in Syria. Both faults are part of the Dead Sea transform fault system, which represents the boundary between the Arabian and African plates and the Levantine subplate. The lavas are made up of about 15–25 vol.% olivine (Fo_{79-84}), 30–40 % clinopyroxene (salite), 40–50 % plagioclase (An_{58-67}), and opaque Fe–Ti oxides (~5 %). Geochemically, they exhibit a narrow range of SiO_2 (44.6 to 47.0 wt %), and MgO (2.9 to 7.5 wt %), are relatively enriched in TiO_2 (2.0 to 2.9 wt %), and are classified as alkali basalts. Mg-numbers range from 0.32 to 0.59, with an average of 0.47. The rocks are enriched in incompatible trace elements such as Zr (98–184 ppm), Nb (16–39 ppm) and Y (25–34 ppm). The REE patterns are fractionated ($(La/Yb)_N = 8.2$), and are generally parallel to subparallel. Such compositions are typical of those of HIMU-OIB and plume-related magmas. Elemental ratios such as K/P (2.9), La/Ta (21.8), La/Nb (0.80), Nb/Y (0.92) and Th/Nb (0.35), and the low average SiO_2 content (46.1 wt %) suggest that the magma was subjected to minimal crustal contamination. This may be related to a rapid ascent of the parental magma, in agreement with the nature (mafic, oceanic crust-like) and the thickness (only about 12 km) of the crust of the Eastern Mediterranean region. Cenozoic volcanism in this region is interpreted to have occurred in association with an episode of localized extension, particularly at the junction between the Yammouneh restraining bend and the Dead Sea–Ghab Transform (that is, in a transtensional tectonic regime). The $^{143}Nd/^{144}Nd$ isotopic composition of the basaltic rocks of northern Lebanon ranges from 0.512842 to 0.512934 ($\varepsilon_{Nd} = 4.0$ to 5.8), and $^{87}Sr/^{86}Sr$ from 0.703317 to 0.703579, suggesting a HIMU-like mantle source. Modelling indicates that the magma was produced by a small degree of partial melting (F = 2 %) of a primitive, garnet lherzolitic mantle source, possibly containing a minor spinel component.

Keywords: Pliocene, alkali basalts, Lebanon, Nd-Sr, petrogenesis, transtension.

1. Introduction

Large discontinuous exposures of basaltic lava flows, ranging in age mostly from Miocene to Recent, are present in several localities extending from Sinai, Jordan, Palestine, Israel, to Lebanon and Syria (Dubertret, 1955; Baldridge *et al*. 1991; Mouty *et al*. 1992; Heimann *et al*. 1996; Shaw *et al*. 2003). These form the Cenozoic volcanic province of the Middle East, occurring mostly along or near the transform faulted boundary (the Dead Sea–Ghab transform fault system) between the Arabian and African plates and the Levantine subplate (Fig. 1). Further to the south, several other extensive Cenozoic volcanic provinces occur in Arabia and east Africa (mostly Ethiopia).

The Cenozoic continental flood basalts in Ethiopia, Yemen, western Arabia and Jordan have been extensively studied (Camp & Roobol, 1989, 1992; Altherr, Henjes-Kunst & Baumann, 1990; Stein & Hofmann, 1992; Baker, Thirlwall & Menzies, 1996; Baker *et al*. 1997; Shaw *et al*. 2003). The Cenozoic volcanic province of Ethiopia is clearly related to the East-African rift system (Barberi *et al*. 1975; Mohr, 1983). The Quaternary intraplate basaltic volcanic field in Yemen appears to be the result of melting shallow mantle, perhaps in response to small amounts of lithospheric extension that were metasomatized and hydrated by the Afar plume during, or shortly after, Oligocene flood volcanism (Baker *et al*. 1997). The lavas of this basaltic field of western Yemen were subjected to variable degrees of contamination (0–20 %) of an Early Proterozoic to Late Archaean silicic lower crustal component (Baker, Thirlwall & Menzies, 1996; Baker *et al*. 1997).

The Cenozoic continental flood basalt provinces of Saudi Arabia may be related to large-scale extension, in association with the development of the rifted margin between the Arabian and the African plates during the opening of the Red Sea (Camp & Roobol, 1989; Camp, Roobol & Hooper, 1992). Camp & Roobol (1992) demonstrated that continental magmatism in western Arabia occurred in two distinct phases; phase

* Author for correspondence: arahman@aub.edu.lb

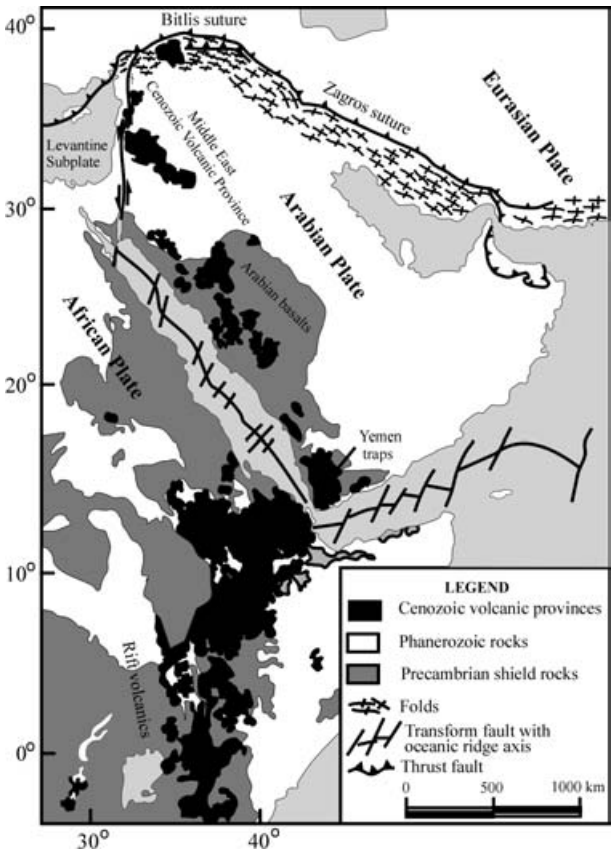

Figure 1. Regional geological map showing the distribution of the various Cenozoic volcanic provinces in east Africa, Arabia and the Middle East.

one from 30 to 20 Ma, produced tholeiitic to transitional lavas, and phase two (12 Ma to Recent) produced transitional to strongly alkalic lavas. Camp & Roobol (1992) related these two magmatic phases to passive-mantle upwelling during extension of the Red Sea basin (for phase one), and to active-mantle upwelling facilitated by minor continental extension (for phase two). White & McKenzie (1989) and Camp & Roobol (1992) indicated that the source of upwelling is either a mantle plume centrally located beneath the West Arabian Swell, or an elongated and extended lobe of hot asthenosphere emanating from the Ethiopian mantle plume. The Ethiopian rift appears to be the only arm of the Afar triple junction which can unambiguously be considered the sole product of active-mantle upwelling, contemporaneous with active-mantle upwelling beneath the West Arabian Swell. It should be noted that, of the three rift arms comprising the Afar triple junction, the Red Sea and Gulf of Aden rifts were well developed by 20 Ma as the result of passive-mantle rifting; in contrast, the Ethiopian rift did not develop until about 10 Ma, shortly after the initiation of significant crustal uplift along the crest of the Afro-Arabian Dome (Bohannon *et al*. 1989).

According to Shaw *et al*. (2003), the source of the alkali basalts and basanites of the Miocene to Recent volcanic field of Jordan was related to melts of deep garnet-bearing asthenosphere, mixed with lithospheric mantle melts. These basaltic mantle melts were formed in response to a phase of lithospheric extension. Shaw *et al*. (2003) concluded that the Afar plume of Ethiopia has not been channelled northwestwards beneath the Arabian plate, and played no role in producing the Arabian or Jordanian volcanic fields.

Baldridge *et al*. (1991) demonstrated that the Miocene basaltic magmatism of Sinai is related to the opening of the Red Sea. The northern extension of the Red Sea rift is represented by the Dead Sea–Ghab transform fault system, along which the investigated basaltic rocks of northern Lebanon were erupted (Figs 1, 2). Some, mostly geochronological and tectonic, studies have been carried out on basaltic rocks from the Cenozoic volcanic province of the Middle East (Syria, the Golan Heights and northern Israel: Garfunkel, 1989; Heimann & Steinitz, 1989; Mouty *et al*. 1992; Mor, 1993; Heimann *et al*. 1996). However, those cropping out in Lebanon have received little attention.

In his discussion of the tectonic setting of the Phanerozoic magmatism in Israel, Garfunkel (1989) described some Cenozoic basalts (known as the 'Cover' basalts, which are located in the southeastern Galilee and in the southern parts of the Golan Heights), as mostly alkaline basalts with some tholeiites, of intraplate character, with ocean island basalt affinities, and proposed that the Jordan Valley depression could have acted as a route for magma ascent. These 'Cover' basalts were dated by Heimann *et al*. (1996), who reported K–Ar ages ranging from 5.5 ± 0.2 Ma to 3.5 ± 0.3 Ma. Using the Ar–Ar method, Heimann & Steinitz (1989) dated some basaltic rocks from the Hula Valley of the Dead Sea rift at 1.4 to 1.1 Ma. The geochronological study of Mor (1993) on the 'Bashan Group' basaltic rocks exposed in northern Israel and in the Golan Heights produced K–Ar ages ranging from Lower Pliocene (5.0 to 3.5 Ma) to Upper Pleistocene (0.4 to 0.1 Ma). Mor (1993) also reported ages ranging from 2.9 to 1.7 Ma (K–Ar ages) for the Mechki basalts of Israel. Weinstein, Navon & Lang (1994) studied some Pleistocene volcanic rocks from the northern Golan Heights, and indicated that these consist of flows and scoria cones of basanite, hawaiite and alkali basalt. The more evolved magmas may have experienced up to 30 % fractionation of clinopyroxene and olivine.

In their general study on Mesozoic and Cenozoic volcanism in Syria, Mouty *et al*. (1992) presented preliminary geochemical data and produced whole-rock K–Ar ages for 43 basaltic samples, with ages ranging from 127.5 ± 2.9 Ma to 1.5 ± 0.1 Ma. They demonstrated that there was a large gap (between 16 and 8 Ma) in Cenozoic volcanic activity, and interpreted this to correspond with the interval between the two

https://doi.org/10.1017/S0016756804009604 Published online by Cambridge University Press

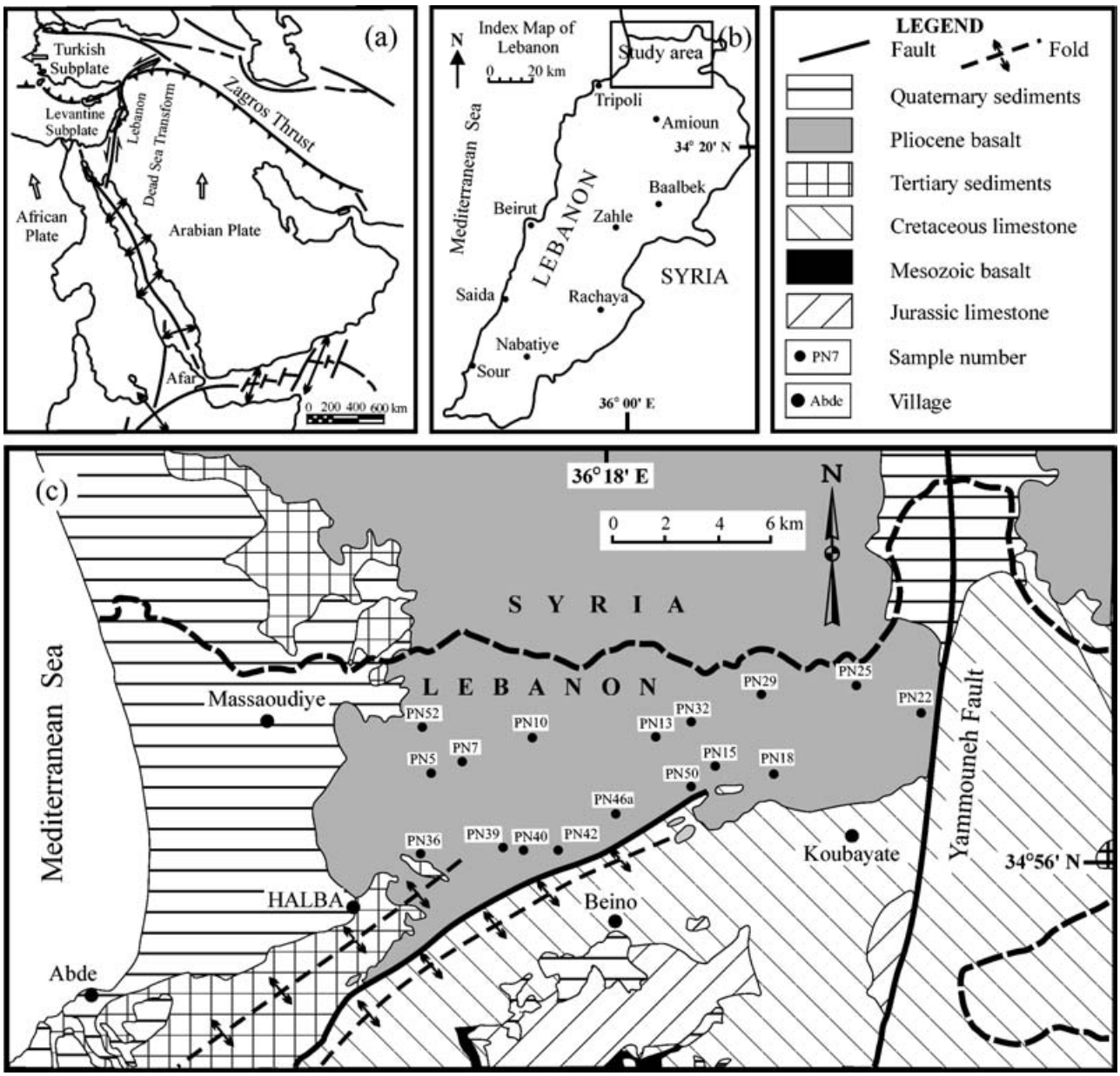

Figure 2. Simplified geological map of northern Lebanon (map c, after Dubertret, 1955) showing locations of the basaltic samples analysed in this study. (a) shows the main structural–tectonic elements in the region, and (b) shows the area of study.

stages of spreading of the Red Sea–Dead Sea rift system. Mouty *et al*. (1992) demonstrated that the rocks are mostly within-plate transitional to alkaline basalts, and that magmatism was associated with left-lateral movements along the Dead Sea rift.

Ages obtained for the Middle East Cenozoic volcanic province range mostly from 26 Ma to 0.1 Ma (K–Ar ages; Raad, 1979; Lang & Steinitz, 1987; Baldridge *et al*. 1991; Mouty *et al*. 1992; Mor, 1993; Butler, Spencer & Griffiths, 1997). In Lebanon, Dubertret (1955) considered the Neogene and Quaternary volcanic rocks in the Akkar and Homs areas to be fissure-type eruptions. He stated that lava ascended along reactivated, as well as recent, fault planes, with the outpouring of large quantities of lava forming voluminous flows. Raad (1979) described some volcanic rocks in the Akkar area as continental alkali-olivine basalts, and dated these basalts (using the K–Ar method) at 4.6 ± 0.23 Ma. He dated some basaltic flows from southern Lebanon (near Hasbaya village) at 2 ± 0.2 Ma. Raad (1979) also described basaltic lavas cropping out near the town of 'Hermel' (located some 30 km southeast of the study area) as blocky lava, and dated these at 7.5 Ma (K–Ar method). Butler, Spencer & Griffiths (1997) described a sequence of basaltic flows at Wadi Shadra (the easternmost part of the investigated volcanic field), and obtained K–Ar ages ranging from 5.7 ± 0.5 Ma to 5.2 ± 0.2 Ma for these flows.

The petrology and geochemistry of the Cenozoic volcanic rocks of Lebanon have not been investigated in

https://doi.org/10.1017/S0016756804009604 Published online by Cambridge University Press

any detail, and the tectonic setting of the magmatism is yet to be determined. The purpose of this contribution is to present a detailed mineralogical, chemical and isotopic study of the Pliocene basalts of northern Lebanon, to evaluate their mantle source characteristics and evolution, and to assess the tectonic setting of magma generation in the context of the regional geodynamic framework.

2. The geological context

Two major volcanic episodes have been identified in the Middle East: a Late Jurassic–Early Cretaceous (Mesozoic) episode, and a Late Cenozoic episode (Dubertret, 1955; Raad, 1979; Lang & Steinitz, 1989; Shimron & Lang, 1989; Garfunkel, 1989, 1998; Mouty *et al*. 1992; Weinstein, Navon & Lang, 1994; Heimann *et al*. 1996; Laws & Wilson, 1997; Abdel-Rahman, 2002).

Cenozoic volcanism in Lebanon followed a long period of transgression and associated carbonate deposition, which took place during most of the Mesozoic and Early Cenozoic. The investigated Pliocene volcanic field is located in the 'Akkar' region of northern Lebanon, between latitudes 34° 32′ and 34° 38′ north, and longitudes 36° 05′ and 36° 20′ east, and is bounded by the Yammouneh transform to the east and the Mediterranean Sea to the west (Fig. 2). This volcanic field covers an area of about 180 km^2 and extends further north into Syria encompassing a larger area of basaltic lava flows, known as the 'Homs' basalts. The Akkar crustal segment has the largest, thickest and most well-preserved Cenozoic volcanic section in Lebanon.

Basalts in the Akkar area form a thick sequence of lava flows: individual flows range in thickness from 1.2 to 4.0 m. Volcanic exposures consist of numerous flows reaching up to 200 m in thickness. The basaltic flows overlie a 3.5 km thick Mesozoic carbonate sequence (Dubertret, 1955; Abdel-Rahman & Nader, 2002). This sequence is part of a much larger Jurassic–Cretaceous carbonate platform deposited in the Neotethys ocean at the northwestern margin of the Arabian Plate, covering a large part of the Eastern Mediterranean region. More specifically, the Akkar basaltic flows overlie sedimentary rocks of the 'Sannine' Formation. This consists of a Middle Cretaceous, thick (0.5–0.6 km) sequence of creamy white, monotonous limestone and dolostone, containing some marl intercalations and chert nodules (Dubertret, 1955; Saint-Marc, 1974; Abdel-Rahman & Nader, 2002). The investigated rocks occur mostly as sub-horizontal to gently dipping, compact, sub-aerial basaltic flows and minor sills, and exhibit variable degrees of vesicularity. Several lava flows are columnar jointed and some exhibit spheroidal weathering. The rocks are generally fresh. Unlike the Mesozoic basalts, the Cenozoic flows do not contain pyroclastic materials. Basaltic dykes intruding carbonate sediments and containing limestone xenoliths of variable size are occasionally present.

Structurally, the Lebanese crust is cross-cut by the major NE–SW-trending Yammouneh fault, which is part of the Dead Sea transform fault plate boundary (Fig. 2a, c). Its northern extension, the Ghab transform of Syria, extends up to, and apparently joins, the continental collision zone at the left-lateral East Anatolian Fault and the Bitlis suture of SE Turkey (Figs 1, 2a). This Dead Sea–Ghab transform fault system shows a sum of 100–105 km of left-lateral Neogene motion (Garfunkel, 1981), and is considered to have been active in Late Cenozoic times during the eruption of the Pliocene basalts of northern Lebanon.

3. Analytical procedures

Analyses of olivine, pyroxene and plagioclase were conducted using a CAMECA Camebax (model MBI) electron microprobe at McGill University, Canada. Counts were obtained simultaneously from four wavelength-dispersion X-ray spectrometers, with a 15 KeV accelerating voltage, a 5 μm beam, and a beam current of 20 nA. Repeated analyses of analytical standards were made to ensure statistical accuracy. On-board software provided by Cameca was used for ZAF corrections and reduction of data. The detection limit for the elements analysed is 0.2 wt %.

Concentrations of the major elements were determined on fused lithium-metaborate discs by X-ray fluorescence spectrometry (Philips PW 1400 Spectrometer at McGill University) using a Rh tube operated at 40 kV and 70 mA. Loss on ignition (LOI) was determined by heating powdered samples for 50 minutes at 1000 °C.

Concentrations of Ni, Cr, Sc, V and Ba were also determined on fused discs along with the major elements as described above. Concentrations of Rb, Sr, Zr, Y, Nb, Ga, Pb, U and Th were determined on pressed pellets by X-ray fluorescence (operating conditions: Rh radiation, 70 kV, 40 mA). The analytical precision, as calculated from 20 replicate analyses of one sample, is better than 1 % for most major elements and better than 5 % for most trace elements.

Concentrations of fourteen rare-earth elements (REE; La to Lu, all except Pm) as well as Hf and Ta were determined by ICP-MS at the Memorial University of Newfoundland, Canada. A pure quartz reagent blank and several certified geological reference standards, as well as internal laboratory standards, were analysed with these samples. Full details of the procedure are given in Longerich *et al*. (1990). Detection limits and reagent blanks are generally about 10 % of chondrite values. The primitive mantle values used for normalization are those of Sun & McDonough (1989).

Sm–Nd isotopic analyses were performed at the GEOTOP Laboratory of the Université du Québec à

https://doi.org/10.1017/S0016756804009604 Published online by Cambridge University Press

Montreal. Between 100 and 150 mg of powder were weighed in a high-pressure teflon vessel and mixed with a ^{149}Sm–^{150}Nd spike and HF–HNO_3 acids. The mixture was dissolved under pressure at 150 °C for one week. The resulting solution was passed through a cationic exchange resin from which the REE were recovered. Sm and Nd were subsequently separated from the other REE using a teflon powder coated with bis-2-orthophosphate acid (HDEHP) following the procedure of Richard, Shimizu & Allègre (1976). The isotopic ratios were measured on a VG Sector-54 mass spectrometer in double-filament mode with Sm and Nd samples loaded on a Ta side filament with a central Re filament. During the course of this study, the La Jolla Nd standard gave $^{143}Nd/^{144}Nd = 0.511848 \pm 16$ (2σ on 34 analyses). The precision on the concentrations and the $^{147}Sm/^{144}Nd$ ratio is better than 1 %, and total blanks for Nd or Sm were < 50 pg. For the Sr isotope analysis, the sample powders were leached in 6M HCl for several hours before commencing the chemical procedures. Sr isotope ratios were measured on the same mass spectrometer described above. Errors for the $^{87}Sr/^{86}Sr$ isotopic ratios are 2σ mean on in-run statistics and correspond to least significant digits; repeat analyses of the NBS SRM 987 gave results of 0.710241 ± 15.

4. Petrography and mineral chemistry

The Pliocene basalts of northern Lebanon are predominantly phyric, with phenocrysts forming 18 to 40 vol.% of the rock. The major phenocryst phases are olivine and clinopyroxene, with some rocks also containing plagioclase phenocrysts. The phenocryst phases are embedded in a microcrystalline to cryptocrystalline groundmass, consisting primarily of plagioclase laths, small grains of clinopyroxene, olivine and opaque iron oxides, in addition to minor amounts of alteration products. The basaltic rocks exhibit a variety of textures including porphyritic, glomeroporphyritic, ophitic, sub-ophitic, intersertal, pilotaxitic and rarely aphyric.

Olivine (15–25 vol.% of the rock) forms subhedral to euhedral, large, equant and occasionally skeletal phenocrysts, as well as minute anhedral groundmass crystals. Corroded and embayed olivine phenocrysts are not uncommon. The olivine phenocrysts are largely fresh, but in some rocks the olivine is partially altered to iddingsite. Clinopyroxene (30–40 vol.% of the rock) is also abundant both as a phenocryst and as a groundmass phase. The proportions of the clinopyroxene existing as phenocryst versus groundmass phases are highly variable. The clinopyroxene forms neutral to pale brown, subhedral to anhedral crystals, occasionally containing inclusions of plagioclase microlaths and opaque phases. Plagioclase makes up about 40 to 50 vol.% of the rock, occurring mostly as groundmass material (0.1 to 0.4 mm long microlaths), and rarely as microphenocrysts or phenocrysts (0.6 to 1 mm long).

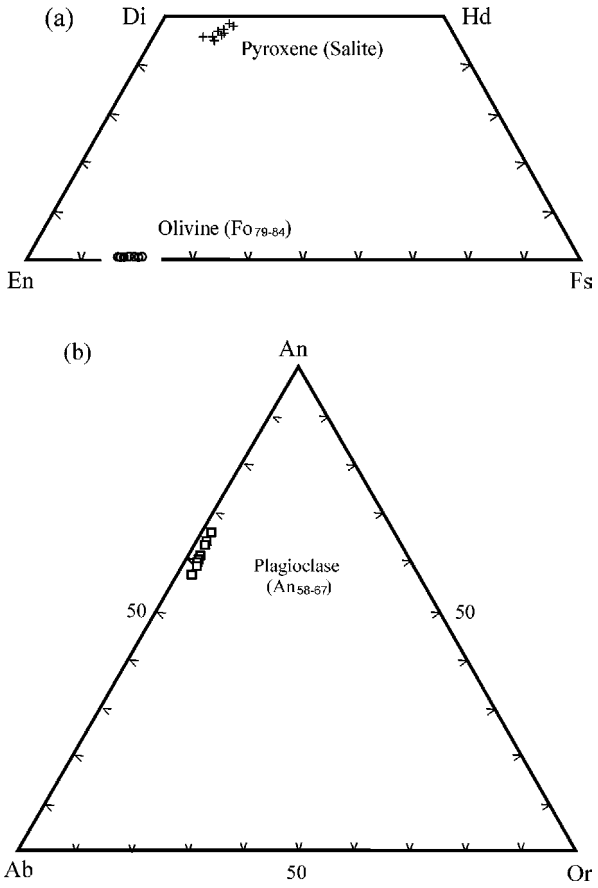

Figure 3. Compositional variations in pyroxene, olivine and plagioclase from the Pliocene alkali basalts of northern Lebanon.

Electron-microprobe data for the various mineral phases and their calculated cations per formulae units are presented in Table 1. The olivine ranges from Fo_{79} to Fo_{84} (Fig. 3a), with CaO contents ranging from 0.22 to 0.28 wt %; MnO and NiO values reach up to 0.26 wt %, and 0.17 wt %, respectively (Table 1). The clinopyroxene is salite in composition (Fig. 3a); its Mg-number ($Mg/(Mg + Fe^{2+})$) ranges from 0.74 to 0.83, and CaO content from 21.3 to 22.0 wt % (Table 1). The salite is relatively enriched in Ti (1.35–2.86 wt % TiO_2) and in Al (2.34–6.01 wt % Al_2O_3). This is typical of clinopyroxene in alkali basaltic lavas (e.g. Dobosi, 1989). Data for plagioclase indicate that it is labradoritic in composition, with An-contents varying from An_{58} to An_{67} (Fig. 3b), and it has a very small Or-component (0.01 to 0.02 K ions per formula unit), but with a somewhat high iron content (0.43 to 0.65 wt % FeO).

5. Geochemistry

5.a. Major, trace and rare-earth element geochemistry

Table 2 contains major and trace element data for 17 representative samples of the Pliocene basaltic rocks of northern Lebanon. They exhibit narrow major

https://doi.org/10.1017/S0016756804009604 Published online by Cambridge University Press

Table 1. Results of electron microprobe analysis and number of cations per formula unit of representative olivine (formulae based on 4O), pyroxene (6O), and plagioclase (8O) from the Pliocene basalts of northern Lebanon

	PN-5	PN-15	PN-22	PN-36	PN-50	PN-5	PN-15	PN-22	PN-36	PN-50	PN-5	PN-15	PN-22	PN-36	PN-50
Sample	Olivine					Pyroxene					Plagioclase				
SiO_2	39.36	38.63	39.01	38.74	39.51	47.92	49.03	47.02	50.47	50.38	52.78	53.60	52.45	52.21	51.73
TiO_2	0.01	0.00	0.02	0.01	0.02	2.86	2.03	2.73	1.35	1.42	0.13	0.13	0.14	0.07	0.06
Al_2O_3	0.17	0.04	0.05	0.04	0.02	4.88	4.12	6.01	2.34	3.65	29.32	28.75	29.76	29.97	30.25
FeO	16.01	18.53	17.50	19.35	16.94	8.88	8.13	8.49	7.89	6.48	0.61	0.50	0.65	0.43	0.45
MnO	0.20	0.24	0.22	0.26	0.00	0.16	0.16	0.16	0.17	0.15	0.00	0.00	0.00	0.00	0.00
MgO	43.73	41.83	42.70	41.10	43.31	12.86	13.69	13.55	14.90	15.43	0.12	0.11	0.07	0.12	0.11
CaO	0.23	0.23	0.22	0.28	0.25	21.95	21.97	21.28	21.39	21.76	12.42	11.81	12.05	13.06	13.41
Na_2O	0.02	0.01	0.02	0.00	0.01	0.49	0.48	0.46	0.39	0.47	4.35	4.66	4.24	3.99	3.77
K_2O	0.00	0.00	0.00	0.00	0.02	0.00	0.00	0.00	0.00	0.00	0.30	0.38	0.28	0.19	0.19
Cr_2O_3	0.02	0.01	0.01	0.02	0.00	0.17	0.38	0.14	0.29	0.36	–	–	–	–	–
NiO	0.17	0.15	0.14	0.11	0.00	0.00	0.02	0.01	0.00	0.01	–	–	–	–	–
Total	99.92	99.67	99.89	99.91	100.08	100.17	100.01	99.85	99.19	100.11	100.03	99.94	99.64	100.04	99.97
Si	0.995	0.992	0.994	0.996	1.000	1.772	1.809	1.740	1.869	1.843	2.399	2.433	2.390	2.373	2.355
Ti	0.000	0.000	0.000	0.000	0.000	0.080	0.056	0.076	0.038	0.039	0.004	0.004	0.005	0.002	0.002
Al	0.005	0.001	0.002	0.001	0.001	0.213	0.179	0.262	0.102	0.158	1.571	1.538	1.598	1.605	1.623
Fe	0.339	0.398	0.373	0.416	0.358	0.247	0.226	0.236	0.220	0.178	0.023	0.019	0.025	0.016	0.017
Mn	0.004	0.005	0.005	0.006	0.000	0.005	0.005	0.005	0.005	0.005	0.000	0.000	0.000	0.000	0.000
Mg	1.648	1.601	1.622	1.575	1.633	0.709	0.753	0.748	0.823	0.842	0.008	0.007	0.005	0.008	0.007
Ca	0.006	0.006	0.006	0.008	0.007	0.869	0.869	0.844	0.849	0.853	0.605	0.574	0.588	0.636	0.654
Na	0.001	0.000	0.001	0.000	0.000	0.035	0.034	0.033	0.028	0.033	0.383	0.410	0.375	0.352	0.333
K	0.000	0.000	0.000	0.000	0.001	0.000	0.000	0.000	0.000	0.000	0.017	0.022	0.016	0.011	0.011
Cr	0.000	0.000	0.000	0.000	0.000	0.005	0.011	0.004	0.008	0.010	–	–	–	–	–
Ni	0.003	0.003	0.003	0.002	0.000	0.000	0.001	0.000	0.000	0.000	–	–	–	–	–
Total	3.001	3.006	3.006	3.004	3.000	3.934	3.944	3.949	3.942	3.961	5.010	5.007	5.002	5.003	5.002

Table 2. Major and trace element composition (in wt %, and ppm, respectively) of representative samples of the Pliocene basalts of northern Lebanon ($Fe_2O_3^*$ is total iron presented as Fe_2O_3, and mg-no. = (molar Mg/(Mg + Fe^{2+})) assuming $Fe^{3+}/Fe^{2+} = 0.15$.)

Sample	PN-5	PN-7	PN-10	PN-13	PN-15	PN-18	PN-22	PN-25	PN-29	PN-32	PN-36	PN-39	PN-40	PN-42	PN-46a	PN-50	PN-52
SiO_2	46.88	47.02	46.45	45.44	46.56	45.70	45.43	44.56	46.59	46.30	46.51	46.07	47.02	45.35	45.46	47.00	46.00
TiO_2	2.63	2.57	2.45	2.37	2.80	2.49	2.94	2.51	2.41	2.29	2.12	2.04	2.09	2.50	2.39	2.27	2.20
Al_2O_3	15.28	15.48	15.92	16.64	15.91	17.09	14.98	15.59	14.83	15.27	14.86	15.03	15.35	16.44	17.67	15.88	15.90
$Fe_2O_3^*$	14.09	14.02	13.96	13.63	13.56	14.63	13.39	14.01	13.44	12.63	13.00	12.15	14.55	14.46	14.36	13.63	14.75
MgO	5.90	5.68	4.69	4.94	4.37	3.80	6.23	6.34	7.10	5.30	7.53	7.45	6.82	3.90	2.86	4.57	5.01
MnO	0.17	0.15	0.16	0.17	0.16	0.17	0.15	0.19	0.16	0.27	0.16	0.14	0.18	0.17	0.17	0.13	0.15
CaO	9.64	9.58	9.57	9.95	7.64	7.63	8.53	9.72	9.93	11.06	8.69	8.79	9.73	8.83	6.41	9.04	8.60
Na_2O	3.18	3.16	2.92	2.80	3.06	2.92	2.74	2.48	2.93	3.16	2.94	2.83	3.14	2.77	2.87	3.06	2.78
K_2O	0.93	0.83	0.76	0.84	1.11	0.73	1.06	1.15	0.96	0.86	0.79	0.74	0.56	0.77	0.82	0.83	0.57
P_2O_5	0.63	0.59	0.52	0.92	0.47	0.34	0.48	0.58	0.48	0.52	0.35	0.35	0.29	0.43	0.34	0.38	0.29
LOI	0.91	1.51	2.42	2.69	4.45	4.98	3.98	2.69	1.51	2.68	2.99	4.63	0.75	4.09	6.66	3.29	3.94
Total	100.24	100.59	99.82	100.39	100.09	100.48	99.91	99.82	100.34	100.34	99.94	100.22	100.48	99.71	100.01	100.08	100.19
Sc	29.0	24.0	27.0	31.0	20.0	25.0	22.0	21.0	25.0	24.0	27.0	27.0	32.0	36.0	23.0	24.0	27.0
V	244.0	254.0	260.0	261.0	246.0	254.0	267.0	238.0	250.0	237.0	215.0	216.0	233.0	257.0	214.0	244.0	266.0
Cr	254.0	270.0	270.0	218.0	228.0	285.0	314.0	304.0	326.0	218.0	255.0	233.0	307.0	215.0	177.0	298.0	346.0
Ni	146.0	134.0	89.0	86.0	96.0	111.0	173.0	228.0	169.0	85.0	114.0	99.0	203.0	96.0	62.0	107.0	191.0
Rb	12.4	11.3	8.1	9.2	17.7	8.6	13.2	14.3	13.9	11.3	10.1	9.3	7.3	9.2	10.4	10.4	5.7
Sr	692.5	740.7	639.0	573.8	555.5	443.0	679.3	744.0	606.3	680.4	483.5	410.2	375.1	553.5	417.3	513.4	410.8
Ba	404.0	403.0	393.0	354.0	442.0	313.0	458.0	590.0	361.0	363.0	317.0	250.0	240.0	351.0	352.0	348.0	268.0
Zr	167.2	149.6	149.8	141.3	183.7	131.2	166.9	142.9	153.4	142.8	134.1	116.4	103.5	143.1	154.5	131.5	97.6
Nb	37.4	34.5	33.8	25.4	36.4	18.8	38.6	35.5	29.6	28.7	21.1	20.3	15.7	24.8	23.8	21.5	16.3
Y	29.7	29.1	29.6	33.1	34.4	30.3	28.1	32.9	28.9	28.1	27.8	25.3	27.2	29.1	31.7	28.5	27.3
Ga	21.9	23.1	22.6	23.3	23.9	23.4	22.7	21.1	21.8	21.9	20.9	20.2	22.5	22.9	24.2	22.4	21.0
Pb	3.9	5.3	3.6	6.5	3.4	4.8	3.1	3.4	5.7	2.3	4.5	2.8	4.0	2.9	2.9	2.8	4.6
Th	9.7	10.3	9.8	9.2	9.2	7.8	9.4	11.3	10.4	10.0	8.6	7.1	8.5	8.7	8.1	8.9	7.7
U	5.0	4.8	4.8	5.0	5.3	5.4	4.4	4.7	5.5	5.0	5.5	5.7	6.8	5.6	5.8	5.5	6.1
Hf		3.52			4.86			3.88					2.75				2.74
Ta		1.54			1.24			1.66					0.57				0.45
Mg no.	0.49	0.49	0.44	0.46	0.43	0.38	0.52	0.51	0.55	0.49	0.57	0.59	0.52	0.39	0.32	0.44	0.44

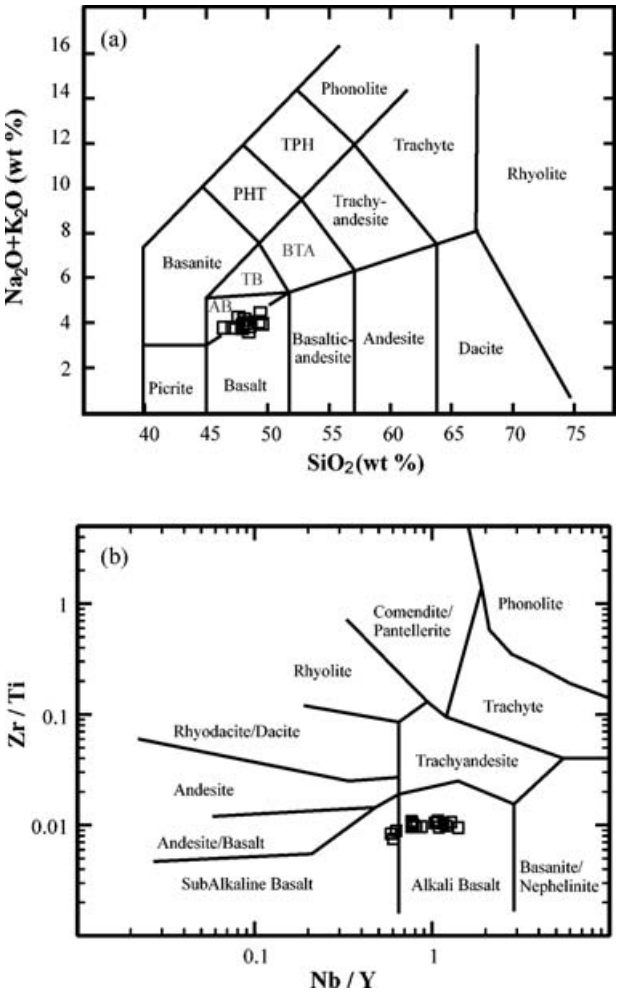

Figure 4. (a) Total alkali–silica (TAS) diagram (after Le Bas & Streckeisen, 1991) showing the classification of the Pliocene volcanic rocks of northern Lebanon, recalculated on an anhydrous basis. Fields are: TPH, tephriphonolite; PHT, phonotephrite; TB, trachybasalt; AB, alkali basalt; BTA, basaltic trachyandesite. (b) Zr/Ti v. Nb/Y diagram (after Winchester & Floyd, 1977) showing that most samples plot in the field of alkali basalt.

element compositional ranges, which vary from 44.6 to 47.0 wt % SiO_2, 14.8–17.7 wt % Al_2O_3, 2.9–7.5 wt % MgO, 12.2–14.8 wt % Fe_2O_3 (as total iron), 6.4–10.0 wt % CaO and 2.0–2.9 TiO_2 (Table 2). In the classification diagram of Le Bas & Streckeisen (1991), data points (recalculated on an anhydrous basis) plot in the field of alkali basalt and overlap with the field of basalt (Fig. 4a). The alkaline nature of the investigated rocks is also indicated in the (Nb/Y)–(Zr/Ti) diagram (Fig. 4b); 14 of the 17 samples plot in the field of alkali basalt. The Mg-numbers (= molar $Mg/(Mg+Fe^{2+})$, assuming a Fe^{3+}/Fe^{2+} ratio of 0.15), are generally low, ranging from 0.32 to 0.59 (with an average of 0.47). Such values indicate that the rocks do not represent primary magmas, but may have experienced some degree of olivine and clinopyroxene fractionation.

The rocks exhibit a relatively narrow trace element compositional range: Cr = 177–346 ppm, V = 214–267 ppm, Sr = 375–744 ppm, Ba = 240–590 ppm, and Rb = 5.7–17.7 ppm. The Pliocene basalts of northern Lebanon are generally enriched in the high field strength elements (HFS) such as Zr (98–184 ppm), Y (25–34 ppm), and Nb (16–39 ppm; Table 2). The investigated rocks exhibit elemental ratios, such as La/Nb (0.80), Zr/Nb (5.4), and Rb/Nb (0.40), similar to average HIMU-OIB (La/Nb = 0.72, Zr/Nb = 4.1 and Rb/Nb = 0.37: Weaver, 1991).

Table 3. Rare earth element (REE) composition (in ppm) of the Pliocene basalts of northern Lebanon

Sample	PN-7	PN-15	PN-25	PN-40	PN-52
La	25.89	27.66	34.43	11.98	12.56
Ce	55.17	59.93	60.55	27.18	26.17
Pr	7.22	7.87	7.66	3.64	3.62
Nd	30.67	34.07	31.68	16.60	16.55
Sm	6.59	7.73	7.17	4.56	4.44
Eu	2.21	2.46	2.33	1.56	1.59
Gd	6.03	7.30	6.54	4.70	4.64
Tb	0.83	1.03	0.94	0.70	0.70
Dy	4.61	5.69	5.26	4.13	4.13
Ho	0.87	1.06	0.99	0.81	0.80
Er	2.20	2.71	2.60	2.19	2.11
Tm	0.29	0.35	0.34	0.29	0.29
Yb	1.77	2.09	1.97	1.74	1.74
Lu	0.25	0.30	0.29	0.25	0.25
∑REE	144.60	160.23	162.74	80.32	79.59

Variation diagrams of major elements versus Zr (Fig. 5) indicate that P_2O_5, TiO_2, alkalis and total iron (as Fe_2O_3) increase gradually with increasing Zr, whereas Al_2O_3 remains somewhat constant. Variations of trace elements versus Zr indicate that they exhibit well-defined trends; Sr, Pb, Th, Nb and Y show a gradual increase with increasing Zr (Fig. 5).

Since Zr and Y are incompatible in the main fractionating phases of basaltic magmas (olivine, pyroxene and plagioclase), the Zr/Y ratio is not normally affected by moderate amounts of fractional crystallization. The variation of Zr/Y with Zr or with FeO can be used to illustrate petrogenetic processes such as partial melting. As Zr is more incompatible in mantle phases than Y, the Zr/Y ratio tends to be higher when the degree of melting is small. Thus, basalts produced by small degrees of partial melting at high pressures have high Zr/Y ratios (and high concentrations of FeO). The positive correlation of Zr/Y with Zr (Fig. 6) suggests that partial melting processes have played a significant role in producing the range of magma compositions observed.

The concentration of the rare-earth elements for five representative samples of the Pliocene alkali basalts of northern Lebanon are given in Table 3. Primitive mantle-normalized REE patterns are illustrated in Figure 7a. The rocks are generally enriched in REE, with the sum of REE ranging from 80 to 163 ppm. Overall, the REE patterns are subparallel, and generally show light rare-earth elements (LREE) enrichment ($(La/Yb)_N = 8.2$). Two of the five samples analysed

https://doi.org/10.1017/S0016756804009604 Published online by Cambridge University Press

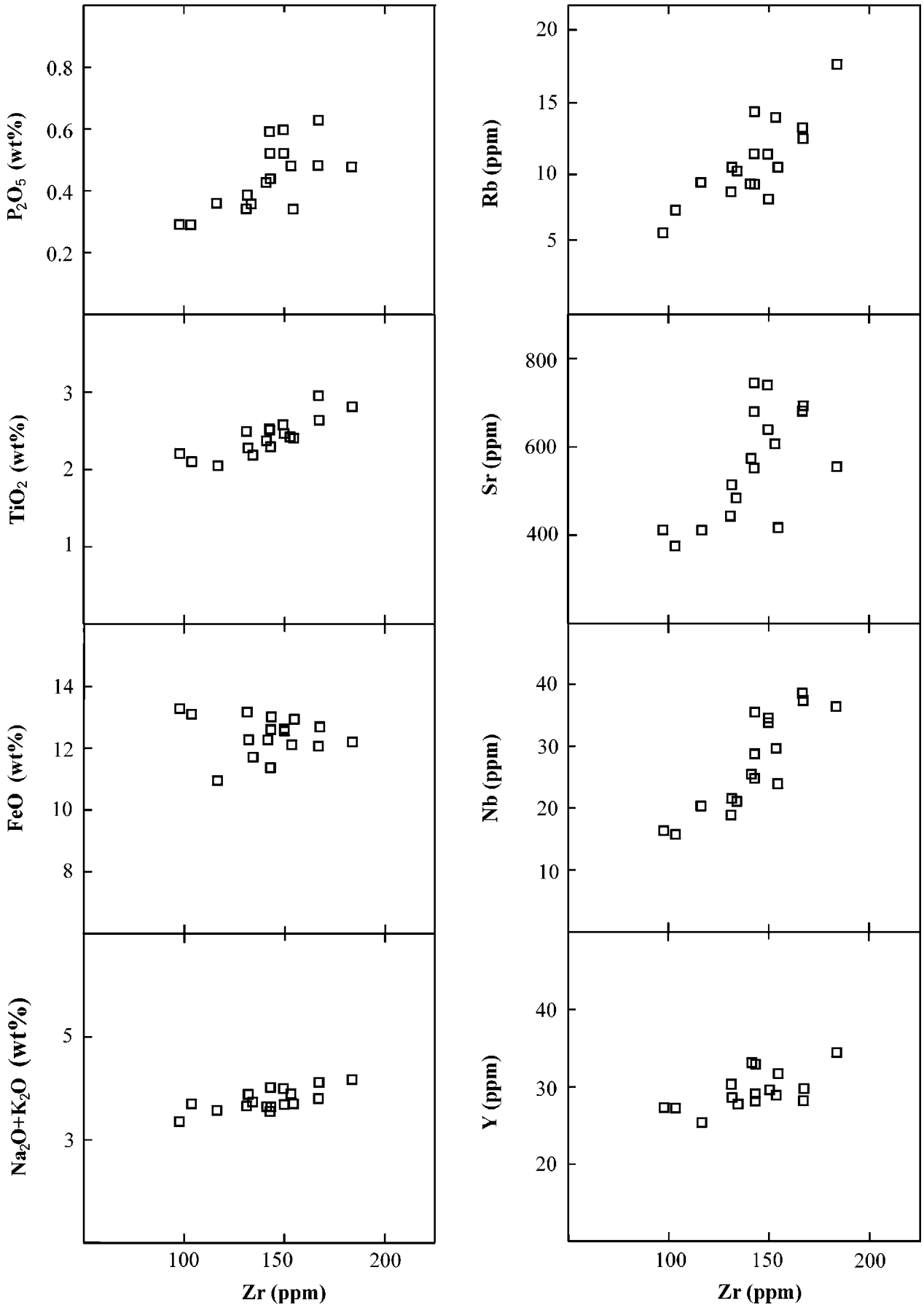

Figure 5. Variations of selected major and trace elements v. Zr within the Pliocene basalts of northern Lebanon.

https://doi.org/10.1017/S0016756804009604 Published online by Cambridge University Press

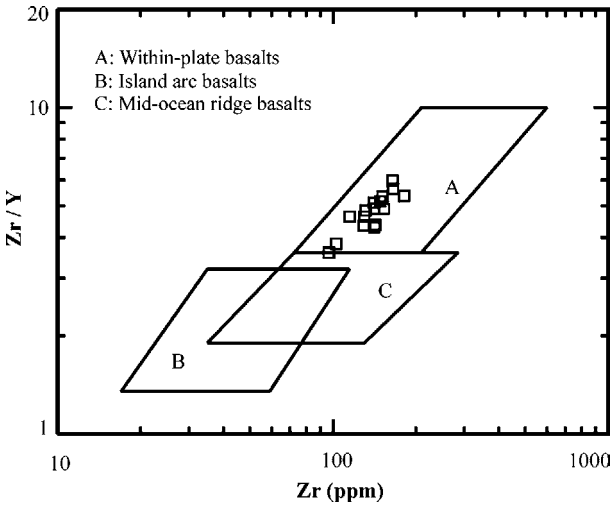

Figure 6. Zr/Y v. Zr variation diagram for the Lebanese Pliocene basaltic rocks. The diagram indicates the within-plate nature of these rocks (fields are after Pearce & Norry, 1979).

Table 4. Sr and Nd isotopic composition of representative samples from the Pliocene basalts of northern Lebanon

Sample	PN-7	PN-15	PN-52
$^{87}Sr/^{86}Sr$	0.703349	0.703579	0.703317
$^{143}Nd/^{144}Nd$	0.512934	0.512842	0.512889
ε_{Nd}	5.77	3.98	4.90

(numbers PN40 and PN52) have significantly lower LREE concentrations than the other samples. This is, most likely, the result of differences in the degrees of partial melting of the mantle source rock, and not due to contamination as confirmed by their isotopic compositions and documented in the Discussion section (see Section 6). In general, enrichment in the LREE is a characteristic feature of OIB-type alkali basalts (e.g. Sun & McDonough, 1989; Weaver, 1991). More specifically, the REE profiles of the investigated basalts (Fig. 7a) are identical to those of the St Helena alkali basalts, which are typical of HIMU-OIB (Chaffey, Cliff & Wilson, 1989). The primitive mantle-normalized incompatible element patterns of the Pliocene alkali basalts of northern Lebanon (Fig. 7b) indicate that the rocks are generally enriched in the incompatible elements compared to primitive mantle abundances. The normalized multi-element profiles of the St Helena alkali basalts generally overlap with those of the Lebanese lavas, but with the latter having higher concentrations of Th (Fig. 7b).

5.b. Rb–Sr and Sm–Nd isotopes

As shown in Table 4, the $^{87}Sr/^{86}Sr$ isotopic compositions of the investigated basalts range from 0.703317 ± 2 to 0.703579 ± 2, and $^{143}Nd/^{144}Nd$ from 0.512842 ± 1 to 0.512934 ± 1 ($\varepsilon_{Nd} = 4.0$ to 5.8). These isotopic compositions are plotted in Figure 8, along

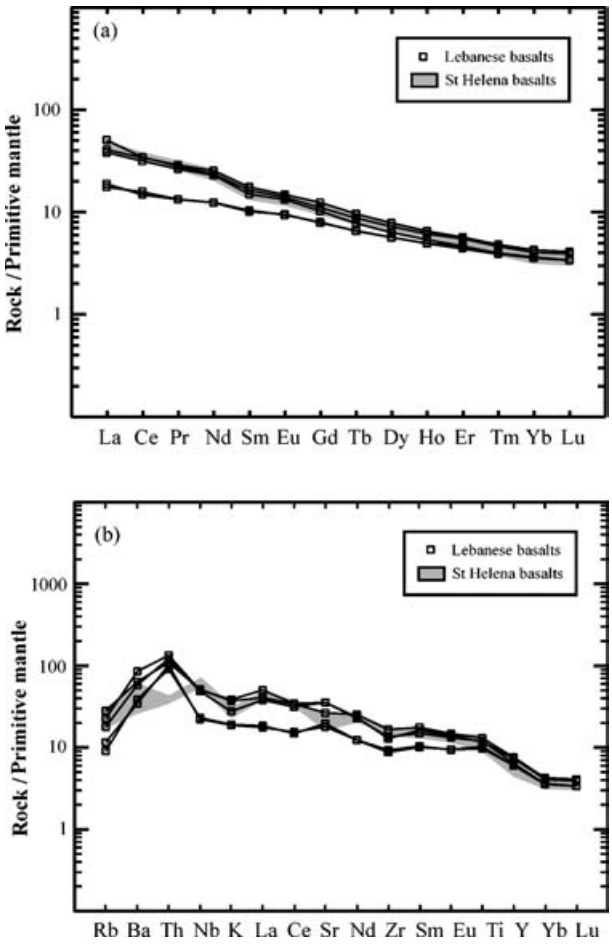

Figure 7. (a) Primitive mantle-normalized rare-earth element (REE) patterns of representative samples from the Pliocene basalts of northern Lebanon, superimposed on an envelope representing the St Helena alkali basalts. (b) Primitive mantle-normalized incompatible element patterns for the Pliocene basalts of northern Lebanon; the St Helena alkali basalts are plotted for comparison. Normalization values used in (a) and (b) are from Sun & McDonough (1989). Data on the St Helena alkali basalts are taken from Chaffey, Cliff & Wilson (1989). Note the similarity of the patterns between the two suites.

with data from other alkali basaltic suites. Also plotted in this diagram (Fig. 8) are the compositions of the various mantle reservoirs (EMI, EMII, HIMU and N-MORB), taken from Hart (1988). It should be noted that HIMU ('high μ') refers to a high $^{238}U/^{204}Pb$ (μ) mantle end-member, and has the lowest $^{87}Sr/^{86}Sr$ of any OIB (Hofmann, 1997), which is thought to be derived from subducted basaltic oceanic crust. EMI ('enriched mantle 1') and EMII ('enriched mantle 2') types of OIB may represent the addition of small amounts of subducted sediments: pelagic in the case of EMI and terrigenous in the case of EMII (Weaver, 1991; Hofmann, 1997). Examples of HIMU-OIB are St Helena, Bouvet, Ascension, Austral Islands, Balleny Islands and the Azores; typical EMI-OIB are Tristan da Cunha, Gough, Kerguelen and Pitcairn; EMII-OIB:

https://doi.org/10.1017/S0016756804009604 Published online by Cambridge University Press

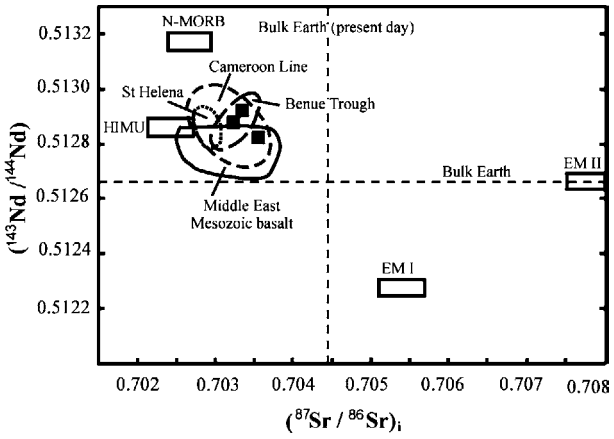

Figure 8. $(^{87}Sr/^{86}Sr)_i$ v. $(^{143}Nd/^{144}Nd)_i$ ratios for the Pliocene basalts of northern Lebanon (closed squares). Compositions of EMI, EMII, HIMU and N-MORB are from Hart (1988). Fields for St Helena from Staudigel *et al*. (1984), Cameroon Line from Halliday *et al*. (1988) and Lee *et al*. (1994), the Benue Trough alkali basalts from Coulon *et al*. (1996), and the Middle East Mesozoic basalts from Laws & Wilson (1997) and Abdel-Rahman (2002). See text for details.

Society Islands, Samoa, Tutuila and Upolu (Weaver, 1991; Hofmann, 1997).

Figure 8 shows that the Pliocene basalts of northern Lebanon are isotopically similar to the plume-related St Helena alkali basalts (Staudigel *et al*. 1984; Hofmann, 1997), to the Benue Trough alkaline basalts of Nigeria (Coulon *et al*. 1996), to the Cameroon Line basalts (Halliday *et al*. 1988, 1990; Lee *et al*. 1994), and to the Mesozoic alkali basalts of the Middle East (Laws & Wilson, 1997; Abdel-Rahman, 2002). The investigated basalts also exhibit isotopic compositions similar to HIMU-OIB (relatively high initial $^{143}Nd/^{144}Nd$ and low initial $^{87}Sr/^{86}Sr$ isotopic ratios), and are thus distinct from EMI-OIB and EMII-OIB (e.g. Weaver, 1991; Wilson, 1993).

6. Discussion

6.a. Nature of the lavas and their source characteristics

In terms of their Zr, Nb and Y compositions (Fig. 9a), the investigated basaltic rocks resemble plume-related mid-ocean ridge basalt (P-MORB), as they exhibit relatively higher concentrations of Nb and Zr, but lower concentrations of Y than transitional-, or normal-MORB (T-MORB or N-MORB; Menzies & Kyle, 1990; Melluso *et al*. 1995). The Sr–Nd isotopic composition of the investigated rocks is similar to that of HIMU-OIB (e.g. Hofmann, 1997), and to the Mesozoic alkali basaltic province of the Middle East, which was also interpreted to be HIMU-like (Laws & Wilson, 1997; Abdel-Rahman, 2002; Fig. 8). The HIMU-OIB lavas of the Cameroon Line, which are isotopically similar to the investigated basalts (cf. Fig. 8), were interpreted to represent small-degree partial melts of

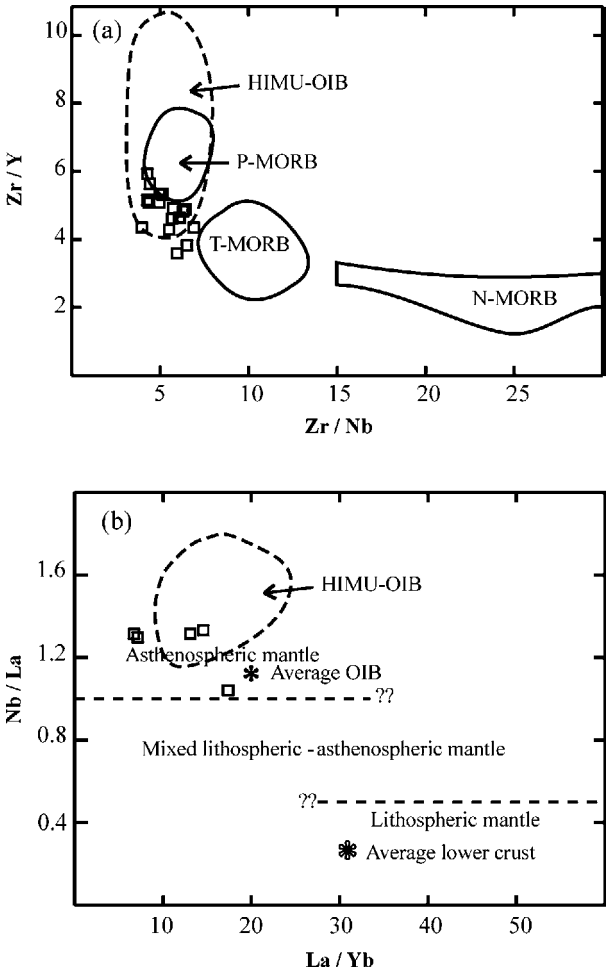

Figure 9. (a) Zr/Y v. Zr/Nb diagram showing that the Pliocene basalts of northern Lebanon plot mostly within the field of HIMU-OIB (taken from Abdel-Rahman, 2002), and in or near the field of fertile, plume-related MORB (P-MORB). The other fields are transitional MORB (T-MORB) and normal MORB (N-MORB) and are taken from Menzies & Kyle (1990). (b) Nb/La v. La/Yb variation diagram. The composition of the Pliocene basalts of northern Lebanon (low La/Yb and high Nb/La) suggests an OIB-like asthenospheric mantle source. Average OIB is after Fitton, James & Leeman (1991), and average lower crust (representing average of six lower crustal granulite xenoliths) is after Chen & Arculus (1995). The field of HIMU-OIB, and the dashed lines separating fields of the asthenospheric, lithospheric and mixed mantle are taken from Abdel-Rahman (2002).

upper mantle material caused by the emplacement of a plume (Halliday *et al*. 1990).

Figure 9a shows also that most of the Pliocene basalts of northern Lebanon plot within the field of HIMU-OIB. Furthermore, the investigated basalts exhibit elemental ratios (Zr/Nb = 5.4, La/Nb = 0.80, Ba/Th = 40, and Rb/Nb = 0.40, on average), similar to those characteristic of HIMU-OIB (Weaver, 1991). Some high field strength (HFS) elements, such as Nb, are found to be highly variable in lithospheric mantle melts. Therefore, the variations in the La/Nb ratios have been interpreted by some authors to reflect the style

https://doi.org/10.1017/S0016756804009604 Published online by Cambridge University Press

of metasomatic enrichment (small fraction convection mantle melt, or subduction-related metasomatism: Gibson *et al*. 1995). In view of the Cenozoic tectonic regime of the Middle East region (tensional to transtensional), subduction-related metasomatism was an unlikely process during that period. Bradshaw & Smith (1994) and Smith *et al*. (1999) have suggested that, since HFS elements (such as Nb) are depleted in the lithospheric mantle relative to the light REE (e.g. La), high Nb/La ratios (approximately > 1) indicate an OIB-like asthenospheric mantle source for basaltic magmas, and lower ratios (approximately < 0.5) indicate a lithospheric mantle source. The Nb/La and La/Yb ratios (averages of 1.26 and 11.9, respectively) are consistent with an asthenospheric mantle (OIB-like) source (Fig. 9b); the investigated basalts plot within or near the field of HIMU-OIB, as also observed in Figure 9a. Thus, trace element and isotopic data suggest that the Pliocene basaltic rocks of northern Lebanon have chemical characteristics similar to HIMU-OIB, derived from the asthenospheric mantle.

The most diagnostic feature of residual garnet is the fractionation of heavy rare-earth elements (HREE; cf. Fig. 7a) owing to their strong partitioning into garnet (McKenzie & O'Nions, 1991). The presence of garnet as a residual phase in the melt source region is inferred from the greater than chondritic Dy/Yb ratio (1.57); the Pliocene alkali basalts of northern Lebanon have an average Dy/Yb ratio of 2.55. These rocks also have $(Tb/Yb)_N$ ratios ranging between 1.72 and 2.11, which are comparable to those of the alkali basalts of Hawaii ($(Tb/Yb)_N$ range from 1.89 to 2.45); the Hawaiian basalts are considered to have been derived from a garnet–lherzolite mantle source (Frey *et al*. 1991; McKenzie & O'Nions, 1991).

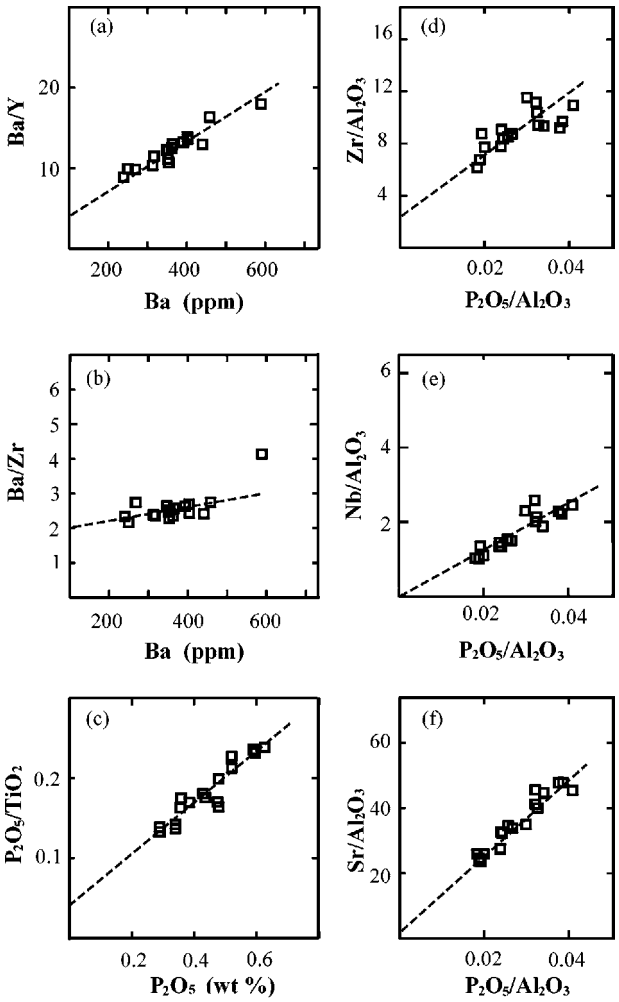

Figure 10. (a, b, c) Plots showing highly/moderately incompatible element ratios v. highly incompatible element concentrations for the Pliocene basalts of northern Lebanon. Zr/Al_2O_3, Nb/Al_2O_3 and Sr/Al_2O_3 v. P_2O_5/Al_2O_3 diagrams (d, e, f, respectively) for the Pliocene basalts of northern Lebanon. See text for details.

6.b. Petrogenetic considerations: role of partial melting

Alkali basaltic rocks are known to be extremely diverse geochemically and derived from diverse mantle sources (e.g. White, 1985; Allègre *et al*. 1987; Hart, 1988; Weaver, 1991; Gibson *et al*. 1997; Abdel-Rahman & Kumarapeli, 1999; Frey *et al*. 2000). The nature of the mantle source material, whether it is dominated by recycled oceanic or continental crust, or by recycled sedimentary components, and the processes associated with melting and migration of melt, determine the composition of the basaltic lavas. In order to assess the role of petrogenetic processes such as fractional crystallization and partial melting in the evolution of mafic lavas, a number of geochemical parameters have been used. For example, during partial melting processes, the highly/moderately incompatible element ratios (such as Ba/Y, Ba/Zr and P_2O_5/TiO_2) are known to decrease with increasing degrees of partial melting (Pankhurst, 1977). The latter demonstrated that partial melting is still by far the most efficient process for fractionating highly/moderately incompatible element ratios. The linear positive trends between these elemental ratios and the concentrations of the highly incompatible elements (Fig. 10a–c) suggest that partial melting may explain variations in the Lebanese Pliocene lavas. The ratio of an element (X) incompatible during melting to Al_2O_3 (which is usually buffered by residual garnet) typically decreases systematically with increasing degrees of partial melting (Hoernle & Schmincke, 1993). The variations of Zr/Al_2O_3, Nb/Al_2O_3, and Sr/Al_2O_3 v. P_2O_5/Al_2O_3 (Fig. 10d–f) define linear trends, mostly passing through or near the origin, which is indicative of the significant role of partial melting processes (e.g. Hoernle & Schmincke, 1993) in producing the range of magma chemistry observed in the investigated basaltic rocks. Thus, the available data suggest that the source of the Pliocene alkali basalts of northern Lebanon was fertile, garnet-bearing, asthenospheric mantle.

https://doi.org/10.1017/S0016756804009604 Published online by Cambridge University Press

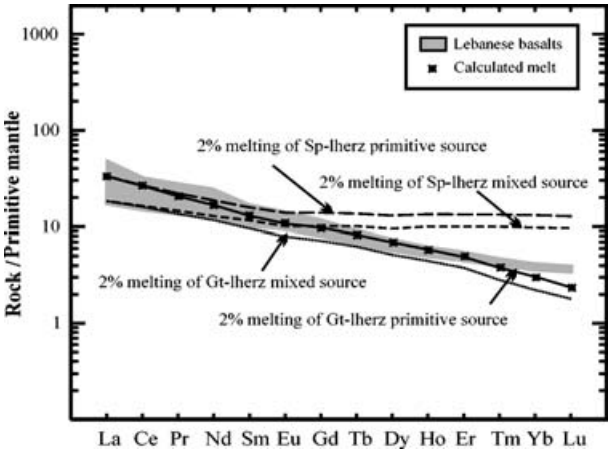

Figure 11. Calculated REE patterns for melts derived by batch partial melting of a primitive mantle composition with REE concentrations from Sun & McDonough (1989) and of a mixed source (50 % primitive/50 % depleted mantle) with REE concentrations from McKenzie & O'Nions (1991). The mantle mineral assemblages and melting proportions used are listed in Table 5. The calculations were made using the Kds of McKenzie & O'Nions (1991), for degrees of partial melting (F) = 1 %, 2 %, and 3 %. Normalization values used are taken from Sun & McDonough (1989). The calculated REE pattern produced by 2 % melting of a primitive garnet lherzolite source matches that of the average Pliocene basalts of northern Lebanon.

To examine the role of partial melting, modelling was performed using the batch melting equations of Shaw (1970). The calculations were done using two model source compositions: (1) primitive mantle taken from Sun & McDonough (1989), and (2) a mixed (50 % primitive–50 % depleted) mantle source of McKenzie & O'Nions (1991). Spinel, garnet and clinopyroxene were assumed to decrease in abundance linearly with increasing degrees of partial melting, as they are typically consumed at less than 25 % partial melting (McKenzie & O'Nions, 1991; Lassiter, DePaolo & Mahoney, 1995). Model and melting proportions are given in Table 5, and are in line with those used in other partial melting calculations (e.g. Hanson, 1980; McKenzie & O'Nions, 1991; Witt-Eickschen & Kramm, 1997). Modelling was performed using three different mantle mineral assemblages: spinel lherzolite, garnet lherzolite and spinel-garnet lherzolite, for both a primitive and a mixed source composition. The partition coefficients used are from McKenzie & O'Nions (1991). Partial melting calculations were performed for 1 %, 2 % and 3 % partial melting. The results of the modelling (Table 5, Fig. 11) show that melting of a spinel-bearing source overestimates the HREE, and melting of a mixed source yields much lower LREE concentrations. Thus, neither depleted nor mixed primitive/depleted mantle material represents the mantle source for the investigated Pliocene basalts, and garnet is a required phase, but possibly with some minor spinel. The REE pattern of the calculated liquid produced by 2 % batch partial melting of garnet lherzolite (of a primitive mantle composition), with the exception of Yb and Lu, produces an excellent fit, as it closely matches that of the average Pliocene basalts of northern Lebanon (Fig. 11). The calculated Yb and Lu contents, however, are lower than the average concentrations of the investigated basalts by 5 % and 11 %, respectively. This may suggest a source within the garnet–spinel transition zone. The study of Watson & McKenzie (1991) indicates that the source of the Hawaiian alkali basalts, which are generally comparable geochemically to the investigated Lebanese basalts, is in the garnet–spinel transition zone. The depth of this transition zone will vary according to mantle potential temperature. It should be noted, however, that Frey, Green & Roy (1978) considered that up to a 15 % difference between calculated and observed melts represented excellent agreement. Some authors argue that accumulated fractional melting rather than batch melting represents the best approximation to melting of the asthenospheric mantle (e.g. Langmuir, Klein & Plank, 1992). However, due to the very small degree of partial melting obtained for the Lebanese basalts, the use of accumulated fractional melting calculations would produce very similar results.

6.c. Role of crustal contamination

Certain chemical parameters can be used to assess the degree of contamination. For example, basaltic rocks affected by crustal contamination exhibit K/P ratios > 7, La/Ta > 22, and La/Nb > 1.5 (e.g. Hart *et al*. 1989). The low values of such elemental ratios in the Pliocene alkali basalts of northern Lebanon (K/P, 2.9; La/Ta, 21.8; La/Nb, 0.80; Nb/Y, 0.92; Th/Nb, 0.35, on average), along with their Sr–Nd isotopic composition, and their low average silica content (46.1 wt % SiO_2), all suggest that the magma was subjected to minimal crustal contamination. Magma ascent may have been rapid enough from the site of partial melting to the surface to escape contamination. As pointed out by Smith *et al*. (1999), the Nd content of most lower crustal xenoliths is too low (usually < 10 ppm) to significantly change Nd-isotopic values without adding 70 % to 85 % lower crustal material. Such large amounts of contamination by crustal material are thermodynamically difficult because a considerable amount of heat is required to assimilate crustal rocks, and the magma would then cool quickly and perhaps 'freeze' in place. Moreover, this would have resulted in the presence of some lower crustal xenoliths within the lava flows, but the investigated Lebanese basaltic flows contain no lower crustal xenoliths.

Based on geological and geophysical data, a number of authors have suggested that the Levantine (including the Lebanese) crust is made up of about 10 km of Phanerozoic sedimentary (mostly carbonate) deposits overlying a 12 km thick, igneous–metamorphic

https://doi.org/10.1017/S0016756804009604 Published online by Cambridge University Press

Table 5. Model parameters and results of batch partial melting calculations using various mineralogical and chemical compositions of primitive and mixed mantle sources

	Starting mode			Melt mode		
Phase	a	b	c	a	b	c
Olivine	0.570	0.550	0.55	0.15	0.05	0.15
Opx	0.235	0.220	0.22	0.15	0.05	0.15
Cpx	0.160	0.160	0.16	0.35	0.30	0.35
Garnet	0.000	0.035	0.07	0.00	0.30	0.35
Spinel	0.035	0.035	0.00	0.35	0.30	0.00

REE	1	2	3	4	5	6	7	8	9	10	11	12	13	14	15	16	17	18	19
La	19.42	12.93	9.69	19.11	12.79	9.61	19.12	12.79	9.61	35.30	23.50	17.61	34.74	23.25	17.46	34.75	17.47	23.25	22.50
Ce	39.83	29.27	23.13	38.85	28.74	22.80	38.35	28.49	22.66	66.64	48.96	38.69	64.99	48.07	38.14	64.16	37.91	47.66	45.80
Pr	5.13	4.05	3.34	4.89	3.91	3.25	4.71	3.79	3.17	7.80	6.16	5.08	7.44	5.94	4.946	7.16	4.83	5.77	6.00
Nd	20.91	17.38	14.86	19.70	16.58	14.30	18.70	15.90	13.82	29.87	24.82	21.23	28.14	23.68	20.43	26.71	19.74	22.71	25.91
Sm	6.01	5.15	4.50	5.33	4.67	4.16	4.78	4.26	3.83	8.21	7.03	6.15	7.28	6.39	5.68	6.53	5.24	5.82	6.10
Eu	1.96	1.72	1.52	1.69	1.52	1.38	1.47	1.35	1.24	2.68	2.35	2.08	2.30	2.07	1.88	2.01	1.69	1.84	2.03
Gd	7.08	6.19	5.50	5.64	5.14	4.71	4.64	4.31	4.02	9.64	8.42	7.48	7.67	6.99	6.42	6.31	5.48	5.87	5.84
Tb	1.26	1.11	0.99	0.92	0.85	0.79	0.71	0.68	0.64	1.68	1.48	1.32	1.23	1.14	1.06	0.95	0.85	0.90	0.84
Dy	8.04	7.13	6.395	5.38	5.09	4.82	3.97	3.83	3.69	10.83	9.59	8.60	7.24	6.85	6.49	5.35	4.97	5.15	4.76
Ho	1.90	1.67	1.49	1.09	1.05	1.01	0.75	0.73	0.71	2.49	2.20	1.96	1.43	1.38	1.32	0.98	0.94	0.96	0.91
Er	5.52	4.86	4.33	2.79	2.73	2.66	1.82	1.80	1.78	7.37	6.49	5.79	3.73	3.64	3.55	2.43	2.38	2.41	2.36
Tm	0.85	0.75	0.66	0.35	0.35	0.34	0.21	0.21	0.21	1.12	0.99	0.88	0.46	0.46	0.45	0.28	0.28	0.28	0.31
Yb	5.42	4.78	4.27	1.85	1.88	1.90	1.08	1.10	1.11	7.42	6.54	5.85	2.53	2.57	2.61	1.48	1.52	1.50	1.86
Lu	0.81	0.72	0.64	0.23	0.24	0.24	0.13	0.13	0.13	1.07	0.95	0.85	0.30	0.31	0.32	0.17	0.17	0.17	0.27

Calculated melts produced by 1 %, 2 %, and 3 % batch partial melting are no. 1 to no. 18, and no. 19 is the measured, average concentration of the Akkar Pliocene basalts.
The starting mode, melt mode, and mantle source type used to produce each of the calculated melts are as follows:
Melt no. 1–3; starting mode a, melt mode a, mixed source, for 1, 2, and 3 % melting, respectively,
no. 4–6; starting mode b, melt mode b, mixed source, for 1, 2, and 3 % melting, respectively,
no. 7–9; starting mode c, melt mode c, mixed source, for 1, 2, and 3 % melting, respectively,
Melt no. 10–12; starting mode a, melt mode a, primitive source, for 1, 2, and 3 % melting, respectively,
no. 13–15; starting mode b, melt mode b, primitive source, for 1, 2, and 3 % melting, respectively,
no. 16–18; starting mode c, melt mode c, primitive source, for 1, 3, and 2 % melting, respectively.
The composition of the calculated melt no. 18 (produced by 2 % melting of garnet lherzolite of a primitive mantle source) closely matches that of the measured average composition of the Akkar Pliocene basalts of northern Lebanon (no. 19). See text for details.

oceanic-like basement complex (Freund *et al*. 1975; Ginzburg & Ben-Avraham, 1987; Ben-Avraham, 1989; Ben-Avraham & Ginzburg, 1990; Khair & Tsokas, 1999). If correct, the presence of such a very thin, mafic, oceanic-like crust in the Eastern Mediterranean region may account for the lack of significant crustal contamination in the Pliocene alkali basalts of northern Lebanon. Thus, the geochemical and field characteristics, along with the nature of the Lebanese crust, suggest that the role of crustal contamination during magma evolution has been minimal.

6.d. Geodynamic considerations

The main tectonic features of the Middle East were created by and are continuously being reshaped as a result of movements of both the African and the Arabian plates. The early geodynamic history of the Middle East, northeast Africa and Arabia indicates that the region was dominated by compressional tectonic regimes during Late Proterozoic time. Voluminous volcanic arc complexes of calc-alkaline affinity were emplaced during the various stages of this compressional tectonic regime (the so-called Pan-African orogenic event; 1100–550 Ma: Abdel-Rahman & Doig, 1987; Abdel-Rahman, 1995). This has resulted in the formation of the Pan-African crust of NE Africa and Arabia, including the southern part of the Levantine region. Thus, the Arabian–Nubian shield was produced at a time when Gondwana was undergoing its final amalgamation by the end of the Late Proterozoic.

The Early Phanerozoic was characterized by extensive fracturing caused by doming, uplift, cooling and relaxation of the newly formed Pan-African crust. Emplacement of anorogenic A-type granitic suites and alkaline ring complexes within the Pan-African crust of eastern Egypt, Sinai, and northwestern Arabia took place during an extended phase of extensional tectonics, spanning nearly the entire Phanerozoic (550 Ma to Present: Abdel-Rahman & Martin, 1990; Abdel-Rahman & El-Kibbi, 2001). During the Mesozoic, tectonism within the Middle East was characterized by the development of a passive continental margin along the northwestern edge of the Arabian Plate in the Eastern Mediterranean region, as micro-continental blocks (present day southern Turkey, Greece and Cyprus) were separated from Gondwana and moved northwards, with the Neotethys ocean opening up behind them (Garfunkel, 1989; Robertson *et al*. 1991). As the continental margin developed, several stages of rifting are believed to have been operative during the Mesozoic era. The main phase of volcanism that produced the Mesozoic alkali basalt province of the Middle East (including the Lebanese Mesozoic basalts) occurred during Jurassic time. The eruption of various Mesozoic alkali basaltic suites within the Middle East may have developed in association with the various stages of Mesozoic extensional tectonics (Garfunkel, 1989, 1998; Gvirtzman, Klang & Rotstein, 1992; Laws & Wilson, 1997; Abdel-Rahman, 2002). The collision of the African–Arabian continent with Eurasia starting in Late Cretaceous time ended the extensional tectonic regime along the Eastern Mediterranean margin, and induced regional compression in the Levant (Laws & Wilson, 1997).

During Miocene time, a major rifting episode culminated in the opening of the Red Sea rift valley. The Dead Sea–Yammouneh–Ghab transform fault system (which represents a plate boundary between the Arabian plate, Sinai and the Levantine subplate) developed at the northern extension of this rift valley. The chemical characteristics of the studied Lebanese Pliocene rocks show that they belong to the within-plate basalt group (cf. Fig. 6), consistent with magma generation in an extensional tectonic regime. Thus, the nature of these rocks, combined with the regional geological context and the overall tectonic framework, suggest that volcanism may have occurred in a localized transtensional regime. This tectonic regime is interpreted to have been developed in association with an episode of localized extension-induced fractures at the junction between the NW-trending restraining bend (the Yammouneh fault) and the northern segment of the Dead Sea–Ghab transform fault system.

The occurrence of such localized tensional forces along the Dead Sea–Ghab fault system is suggested by the presence of several elongate basins of Miocene, Pliocene and younger ages, at several localities along this fault system (e.g. Mart, 1991; Gomez *et al*. 2001; M. Fatfat, unpub. M.S. thesis, American Univ. Beirut, Lebanon, 2001). The regular occurrence of left steppings at elongate basins along this fault zone has been interpreted by Gomez *et al*. (2001) as indicative of a pull-apart mechanism for basin formation. Gomez *et al*. (2001) indicated also that left-lateral striations on fault planes imply a dip-slip component (20–25 %) of the movement along the fault. Mart (1991) considered the Dead Sea rift as the northern extension of the Red Sea spreading centre, and indicated that it is made up of several successive internal basins. He suggested that the tectonic evolution was possibly initiated during Pliocene time, as a result of the clockwise jump of the Red Sea spreading axis. Mart (1991) pointed out that existing information concerning the true nature of the Dead Sea fault is controversial, as it supports both a vertical offset (possible rift) and a regional sinistral horizontal movement (possible transform).

Garfunkel (1989) interpreted the Pliocene volcanic event (that produced the 'Cover' basalts, which are located to the southeast of Galilee and at the southern parts of the Golan Heights), to have been contemporaneous with rifting, continental break-up and regional uplift. He suggested that the Dead Sea transform fault system is a leaky transform, and that it acted as an avenue through which basaltic magma has reached the surface. This is consistent with our interpretation

of the emplacement of the Pliocene basalts of northern Lebanon in a transtensional environment, where localized tensional forces may have occurred at the junction (located near the Lebanese–Syrian border) between the 'Yammouneh' restraining bend and the Ghab transform.

The role of mantle plumes, particularly in the generation of flood basaltic magmas, has been emphasized by many authors. According to Hofmann (1997), mantle plumes are thought to generate about 20–40 stationary hotspots. Plumes probably originate from boundary layers in the mantle, which may be located either above the 660 km seismic discontinuity or above the core–mantle boundary (at 2900 km: Hofmann, 1997). In either case, heating from below lowers the density until the layer becomes unstable and forms a rising column or plume. Shaw *et al*. (2003) concluded that the Afar plume of Ethiopia has not been channelled northwestwards beneath the Arabian plate, and played no role in producing the Arabian or Jordanian volcanic fields. It is not clear whether or not the Lebanese Cenozoic volcanic field is related to a mantle plume, especially because it is volumetrically insignificant compared to the Afar flood basalts, or to the Cenozoic volcanism in Arabia and Jordan.

7. Conclusions

(1) The Pliocene basalts of northern Lebanon represent a significant component of the Cenozoic Volcanic Province of the Middle East. The lavas form relatively thick continuous successions. They are mostly phyric, consisting of about 15–25 vol.% olivine (Fo_{79-84}), 30–40 % clinopyroxene (salite), 40–50 % plagioclase (labradorite; An_{58-67}) and 5 % opaque Fe–Ti oxide phases.

(2) Geochemically, the rocks have a narrow range of major element compositions (SiO_2, 44.6–47.0 wt %; MgO, 2.9–7.5 wt %), are alkaline in nature (cf. Fig. 4) and are enriched in Ti (2.0–2.9 wt % TiO_2), Zr (98–184 ppm), Nb (16–39 ppm) and Y (25–34 ppm). These features reflect strong affinities to OIB. The primitive mantle-normalized patterns are fractionated ($(La/Yb)_N = 8.2$) and conformable. The $^{143}Nd/^{144}Nd$ isotopic composition of the investigated alkali basalts ranges from 0.512842 to 0.512934 ($\varepsilon_{Nd} = 4.0$ to 5.8), and $^{87}Sr/^{86}Sr$ from 0.703317 to 0.703579. The chemical and isotopic compositions of these rocks are similar to those of HIMU-OIB, such as the St Helena alkali basalts.

(3) The overall chemical characteristics suggest that the Pliocene alkali basalts of northern Lebanon were derived from a fertile mantle source. Petrogenetic modelling indicates that the magma was produced by a small-degree partial melting (F = 2 %) of a garnet lherzolite source, possibly containing a minor spinel component.

(4) Elemental ratios such as K/P (2.9, on average), La/Nb (0.8), Nb/Y (0.92) and Th/Nb (0.35) suggest that crustal contamination did not play a significant role during magma evolution; the magmas probably experienced very rapid ascent. This is consistent with the nature (mafic, oceanic-like) and the small thickness (about 12 km) of the crust of the Eastern Mediterranean region.

(5) The Pliocene alkali basalts of northern Lebanon display the geochemical characteristics of within-plate lavas. As inferred from geochemical and tectonic data, volcanism is interpreted to have been associated with a localized transtensional regime, which occurred at the junction between the restraining NW-trending bend (the Yammouneh fault) and the northern segment of the Dead Sea–Ghab transform fault system.

Acknowledgements. Glenna Keating and Pam King are thanked for facilitating the acquisition of the X-ray fluorescence, and the ICP-MS data, respectively. We thank R. Stevensen for his help in obtaining the Sm–Nd and Rb–Sr isotope data at the UQAM GEOTOP laboratory (Montreal), and G. Poirier for his assistance during the electron microprobe work at McGill University. Discussions with S. Nadeau, S. Schmidberger and T. Simonetti are appreciated. We acknowledge the technical support provided by Mr M. Ijreiss. S. Gibson and an anonymous referee are thanked for their reviews, which improved our contribution. Research costs were covered by an AUB-URB grant to Abdel-Rahman.

References

ABDEL-RAHMAN, A. M. 1995. Tectonic-magmatic stages of shield evolution: the Pan-African belt in northeastern Egypt. *Tectonophysics* **242**, 223–40.

ABDEL-RAHMAN, A. M. 2002. Mesozoic volcanism in the Middle East: geochemical, isotopic and petrogenetic evolution of extension-related alkali basalts from central Lebanon. *Geological Magazine* **139**, 621–40.

ABDEL-RAHMAN, A. M. & DOIG, R. 1987. The Rb–Sr geochronological evolution of the Ras Gharib segment of the northern Nubian shield. *Journal of the Geological Society, London* **144**, 577–86.

ABDEL-RAHMAN, A. M. & EL-KIBBI, M. 2001. Anorogenic magmatism: chemical evolution of the Mount El-Sibai A-type complex (Egypt), and implications for the origin of within-plate felsic magmas. *Geological Magazine* **138**, 67–85.

ABDEL-RAHMAN, A. M. & KUMARAPELI, P. S. 1999. Geochemistry and petrogenesis of the Tibbit Hill metavolcanic suite of the Appalachian Fold Belt, Quebec-Vermont: a plume-related and fractionated assemblage. *American Journal of Science* **299**, 210–37.

ABDEL-RAHMAN, A. M. & MARTIN, R. F. 1990. The Mount Gharib A-type granite, Nubian shield: petrogenesis and role of metasomatism at the source. *Contributions to Mineralogy and Petrology* **104**, 173–83.

ABDEL-RAHMAN, A. M. & NADER, F. H. 2002. Characterization of the Lebanese Jurassic–Cretaceous carbonate stratigraphic sequence: A geochemical approach. *Geological Journal* **37**, 69–91.

ALLÈGRE, C. J., HAMELIN, B., PROVOST, A. & DUPRÉ, B. 1987. Topology in isotopic multispace and origin of mantle chemical heterogeneities. *Earth and Planetary Science Letters* **81**, 319–37.

ALTHERR, R., HENJES-KUNST, F. & BAUMANN, A. 1990. Asthenosphere as a possible source for basaltic magmas erupted during the formation of the Red Sea: constraints from Sr, Pb, and Nd isotopes. *Earth and Planetary Science Letters* **96**, 269–86.

BAKER, J. A., MENZIES, M. A., THIRLWALL, M. F. & MACPHERSON, C. J. 1997. Petrogenesis of Quaternary intraplate volcanism, Sana'a, Yemen: implications for plume-lithosphere interaction and polybaric melt hybridization. *Journal of Petrology* **38**, 1359–90.

BAKER, J. A., THIRLWALL, M. F. & MENZIES, M. A. 1996. Sr–Nd–Pb isotopic and trace element evidence for crustal contamination of plume-derived flood basalts: Oligocene flood volcanism in western Yemen. *Geochimica et Cosmochimica Acta* **60**, 2559–81.

BALDRIDGE, W. S., EYAL, Y., BARTOV, Y., STEINITZ, G. & EYAL, M. 1991. Miocene magmatism of Sinai related to the opening of the Red Sea. *Tectonophysics* **197**, 181–201.

BARBERI, F., FERRARA, G., SANTACROCE, R., TREUIL, M. & VARET, J. 1975. A transitional basalt-pantellerite sequence of fractional crystallization: The Boina center (Afar rift, Ethiopia). *Journal of Petrology* **16**, 22–56.

BEN-AVRAHAM, Z. 1989. Multiple opening and closing of the eastern Mediterranean and south China basins. *Tectonics* **8**, 351–62.

BEN-AVRAHAM, Z. & GINZBURG, A. 1990. Displaced terranes and crustal evolution of the Levant and eastern Mediterranean. *Tectonics* **9**, 613–22.

BOHANNON, R. G., NAESER, C. W., SCHMIDT, D. L. & ZIMMERMANN, R. A. 1989. The timing of uplift, volcanism and rifting peripheral to the Red Sea: a case for passive rifting? *Journal of Geophysical Research* **94B**, 1683–701.

BRADSHAW, T. K. & SMITH, E. I. 1994. Polygenetic Quaternary volcanism at Crater Flat, Nevada. *Journal of Volcanology and Geothermal Research* **63**, 165–82.

BUTLER, R. W. H., SPENCER, S. & GRIFFITHS, H. M. 1997. Transcurrent fault activity on the Dead Sea Transform in Lebanon and its implications for plate tectonics and seismic hazard. *Journal of the Geological Society, London* **154**, 757–60.

CAMP, V. E. & ROOBOL, M. J. 1989. The Arabian continental alkali basalt province: Part I. Evolution of Harrat Rahat, Kingdom of Saudia Arabia. *Geological Society of America Bulletin* **101**, 71–95.

CAMP, V. E. & ROOBOL, M. J. 1992. Upwelling asthenosphere beneath western Arabia and its regional implications. *Journal of Geophysical Research* **97B**, 15255–71.

CAMP, V. E., ROOBOL, M. J. & HOOPER, P. R. 1992. The Arabian continental alkali basalt province: Part III. Evolution of Harrat Kishb, Kingdom of Saudia Arabia. *Geological Society of America Bulletin* **104**, 379–96.

CHAFFEY, D. J., CLIFF, R. A. & WILSON, B. M. 1989. Characterization of the St Helena magma sourse. In *Magmatism in the ocean basins* (eds A. D. Saunders and M. J. Norry), pp. 257–76. Geological Society of London, Special Publication no. 42.

CHEN, W. & ARCULUS, R. J. 1995. Geochemical and isotopic characteristics of lower crustal xenoliths, San Francisco Volcanic Field, Arizona, U.S.A. *Lithos* **36**, 203–25.

COULON, C., VIDAL, P., DUPUY, C., BAUDIN, P., POPOFF, M., MALUSKI, H. & HERMITTE, D. 1996. The Mesozoic to Early Cenozoic magmatism of the Benue Trough (Nigeria); geochemical evidence for the involvement of the St Helena plume. *Journal of Petrology* **37**, 1341–58.

DOBOSI, G. 1989. Clinopyroxene zoning patterns in the young alkali basalts of Hungary and their petrogenetic significance. *Contributions to Mineralogy and Petrology* **101**, 112–21.

DUBERTRET, L. 1955. *Carte Geologique du, Liban aux 1/200,000, avec notice explicative*. Ministire des Travaux Public, Beyrouth, 74 pp.

FITTON, J. G., JAMES, D. & LEEMAN, W. P. 1991. Basic magmatism associated with Late Cenozoic extension in the western United States: compositional variations in space and time. *Journal of Geophysical Research* **96**, 13693–712.

FREUND, R., GOLDBERG, M., WEISSBROD, T., DRUCKMAN, Y. & DERIN, B. 1975. The Triassic–Jurassic structure of Israel and its relation to the eastern Mediterranean. *Israel Geological Survey Bulletin* **65**, 26 pp.

FREY, F. A., CLAGUE, D., MAHONEY, J. J. & SINTON, J. M. 2000. Volcanism at the edge of the Hawaiian plume: petrogenesis of submarine alkalic lavas from the North Arch Volcanic Field. *Journal of Petrology* **41**, 667–91.

FREY, F. A., GARCIA, M. O., WISE, W. S., KENNEDY, A., GURRIET, P. & ALBAREDE, F. 1991. The evolution of Mauna Kea volcano, Hawaii: Petrogenesis of tholeiitic and alkali basalts. *Journal of Geophysical Research* **96**, 14347–75.

FREY, F. A., GREEN, D. H. & ROY, S. D. 1978. Integrated models of basalt petrogenesis: a study of quartz tholeiites to olivine melilites from southeastern Australia utilizing geochemical and experimental data. *Journal of Petrology* **19**, 463–513.

GARFUNKEL, Z. 1981. Internal structure of the Dead Sea leaky transform (rift) in relation to plate kinematics. *Tectonophysics* **80**, 181–208.

GARFUNKEL, Z. 1989. Tectonic Setting of Phanerozoic magmatism in Israel. *Israel Journal of Earth Sciences* **38**, 51–74.

GARFUNKEL, Z. 1998. Constraints on the origin and history of the Eastern Mediterranean basin. *Tectonophysics* **298**, 5–35.

GIBSON, S. A., THOMPSON, R. N., DICKIN, A. P. & LEONARDOS, O. H. 1995. High-Ti and low-Ti mafic potassic magmas: key to plume-lithosphere interactions and continental flood-basalt genesis. *Earth and Planetary Science Letters* **136**, 149–65.

GIBSON, S. A., THOMPSON, R. N., WESKA, R. K., DICKIN, A. P. & LEONARDOS, O. H. 1997. Late Cretaceous rift-related upwelling and melting of the Trinidade starting mantle plume head beneath western Brazil. *Contributions to Mineralogy and Petrology* **126**, 303–14.

GINZBURG, A. & BEN-AVRAHAM, Z. 1987. The deep structure of the central and southern Levant continental margin. *Annals Tectonicae* **1**, 105–15.

GOMEZ, F., MEGHRAOUI, M., DARKAL, A. N., SBEINATI, R., DARAWCHEH, R., TABET, C., KHAWLIE, M., CHARABE, M., KHAIR, K. & BARAZANGI, M. 2001. Coseismic displacements along the Serghaya Fault: an active branch of the Dead Sea Fault System in Syria and Lebanon. *Journal of the Geological Society, London* **158**, 405–8.

GVIRTZMAN, Z., KLANG, A. & ROTSTEIN, Y. 1992. Early Jurassic shield volcano below Mount Carmel: New

interpratation of the magnetic and gravity anomalies and implication for Early Jurassic rifting. *Israel Journal of Earth Sciences* **39**, 149–59.

HALLIDAY, A. N., DAVIDSON, J. P., HOLDEN, P., DEWOLF, C., LEE, D.-C. & FITTON, J. G. 1990. Trace-element fractionation in plumes and the origin of HIMU mantle beneath the Cameroon line. *Nature* **347**, 523–8.

HALLIDAY, A. N., DICKIN, A. P., FALLICK, A. E. & FITTON, J. G. 1988. Mantle dynamics: a Nd, Sr, Pb and O isotopic study of the Cameroon Line volcanic chain. *Journal of Petrology* **29**, 181–211.

HANSON, G. N. 1980. Rare earth elements in petrogenetic studies of igneous systems. *Annual Reviews in Earth Sciences* **8**, 371–406.

HART, S. R. 1988. Heterogeneous mantle domains signatures, genesis and mixing chronologies. *Earth and Planetary Science Letters* **90**, 273–96.

HART, W. K., WOLDE, G. C., WALTER, R. C. & MERTZMAN, S. A. 1989. Basaltic volcanism in Ethiopia: constraints on continental rifting and mantle interactions. *Journal of Geophysical Research* **94**, 7731–48.

HEIMANN, A. & STEINITZ G. 1989. $^{40}Ar/^{39}Ar$ total gas ages of basalts from Notera #3 well, Hula Valley, Dead Sea Rift: Stratigraphic and tectonic implications. *Israel Journal of Earth Sciences* **38**, 173–84.

HEIMANN, A., STEINITZ, G., MOR, D. & SHALIV, G. 1996. The Cover Basalt Formation, its age and its regional and tectonic setting: Implications from K–Ar and $^{40}Ar/^{39}Ar$. *Israel Journal of Earth Sciences* **45**, 55–71.

HOERNLE, K. & SCHMINCKE, H. U. 1993. The role of partial melting in the 15 Ma geochemical erosion of Gran Canaria: a blob model for the Canary hotspot. *Journal of Petrology* **34**, 599–626.

HOFMANN, A. W. 1997. Mantle geochemistry: the message from oceanic volcanism. *Nature* **385**, 219–29.

KHAIR, K. & TSOKAS, G. N. 1999. Nature of the Levantine (eastern Mediterranean) crust from multiple-source Werner deconvolution of Bouguer gravity anomalies. *Journal of Geophysical Research* **104**, 25469–78.

LANG, B. & STEINITZ, G. 1987. K–Ar dating of subsurface Mesozoic and Cenozoic magmatic rocks in Israel. *Geological Survey of Israel Report* **GSI/8/87**, 48 pp.

LANG, B. & STEINITZ, G. 1989. K–Ar dating of Mesozoic magmatic rocks in Israel. *Israel Journal of Earth Sciences* **38**, 89–104.

LANGMUIR, C. H., KLEIN, E. M. & PLANK, T. 1992. Petrological systematics of mid-ocean ridge basalts: Constraints on melt generation beneath ocean ridges. In *Mantle Flow and Melt Generation at Mid-Ocean Ridges* (eds J. Phipps Morgan, D. K. Blackman and J. M. Sinton), pp. 183–280. American Geophysical Union, Geophysical Monograph no. 71.

LASSITER, J. C., DEPAOLO, D. J. & MAHONEY, J. J. 1995. Geochemistry of the Wrangellia Flood Basalt Province: implications for the role of continental and oceanic lithosphere in flood basalt genesis. *Journal of Petrology* **36**, 983–1009.

LAWS, E. D. & WILSON, M. 1997. Tectonics and magmatism associated with Mesozoic passive continental margin development in the Middle East. *Journal of the Geological Society, London* **154**, 757–60.

LE BAS, M. J. & STRECKEISEN, A. L. 1991. The IUGS systematics of igneous rocks. *Journal of the Geological Society, London* **148**, 825–33.

LEE, D.-C., HALLIDAY, A. N., FITTON, J. G. & POLI, G. 1994. Isotopic variation with distance and time in the volcanic islands of the Cameroon Line: evidence for a mantle plume origin. *Earth and Planetary Science Letters* **123**, 119–38.

LONGERICH, H. P., JENNER, G. A., FRYER, B. J. & JACKSON, S. E. 1990. Inductively coupled plasma–mass spectrometric analysis of geological samples: A critical evaluation based on case studies. *Chemical Geology* **83**, 105–18.

MART, Y. 1991. The Dead Sea Rift: from continental rift to incipient ocean. *Tectonophysics* **197**, 155–79.

MCKENZIE, D. P. & O'NIONS, R. K. 1991. Partial melting distributions from inversion of rare earth element concentrations. *Journal of Petrology* **32**, 1021–91.

MELLUSO, L., BECCALUVA, L., BROTZU, P., GREGNANIN, A., GUPTA, A. K., MORBIDELLI, L. & TRAVERSA, G. 1995. Constraints on the mantle sources of the Deccan Traps from the petrology and geochemistry of the basalts of Gujarat State (Western India). *Journal of Petrology* **36**, 1393–432.

MENZIES, M. A. & KYLE, R. 1990. Continental volcanism: a crust-mantle probe. In *Continental Mantle* (ed. M. A. Menzies), pp. 157–77. Oxford: Oxford Science Publishers.

MOHR, P. 1983. Ethiopian flood basalt province. *Nature* **303**, 577–84.

MOR, D. 1993. A time-table for the Levant volcanic province, according to K–Ar dating in the Golan Heights. *Journal of African Earth Sciences* **16**, 223–34.

MOUTY, M., DELALOYE, M., FONTIGNIE, D., PISKIN, O. & WAGNER, J.-J. 1992. The volcanic activity in Syria and Lebanon between Jurassic and actual. *Schweizerische Mineralogische und Petrografische Mitteilungen* **72**, 91–105.

PANKHURST, R. J. 1977. Open system fractionation and incompatible element variations in basalts. *Nature* **268**, 36–8.

PEARCE, J. A. & NORRY, M. J. 1979. Petrogenetic implications of Ti, Zr, Y, and Nb variations in volcanic rocks. *Contributions to Mineralogy and Petrology* **69**, 33–47.

RAAD, K. 1979. *Les Formations Volcaniques du Liban*. Docteur 3e cycle, published thesis, Université de Paris-Sud, Centre d'Orsay, France, 114 pp.

RICHARD, P., SHIMIZU, N. & ALLÈGRE, C. J. 1976. $^{143}Nd/^{144}Nd$, a natural tracer: an application to oceanic basalts. *Earth and Planetary Science Letters* **31**, 269–78.

ROBERTSON, A. H. F., CLIFT, P. D., DEGNAN, P. J. & JONES, G. 1991. Palaeogeographic and palaeotectonic evolution of the eastern Mediterranean Neotethys. *Palaeogeography, Palaeoclimatology, Palaeoecology* **87**, 289–343.

SAINT-MARC, P. 1974. Etude stratigraphique et micropaleontologique de l'Albien, du Cenomanien et du Turonien. In *Note et Memoires sur le Moyen-Orient; Tome XIII* (ed. L. Dubertret), pp. 1–342. Paris-Beirut: CNRS.

SHAW, D. M. 1970. Trace element fractionation during anatexis. *Geochimica et Cosmochimica Acta* **34**, 237–43.

SHAW, J. E., BAKER, J. A., MENZIES, M. A., THIRLWALL, M. F. & IBRAHIM, K. M. 2003. Petrogenesis of the largest intraplate volcanic field on the Arabian Plate (Jordan): a mixed lithosphere-asthenosphere source activated by

lithospheric extension. *Journal of Petrology* **44**, 1657–79.

SHIMRON, A. E. & LANG, B. 1989. Cretaceous magmatism along the southern flank of Mount Hermon. *Israel Journal of Earth Sciences* **38**, 125–42.

SMITH, E. I., SÁNCHEZ, A., WALKER, J. D. & WANG, K. 1999. Geochemistry of mafic magmas in the Hurricane Volcanic Field, Utah: implications for small- and large-scale chemical variability of the lithospheric mantle. *Journal of Geology* **107**, 433–48.

STAUDIGEL, H., ZINDLER, A., HART, S. R., LESLIE, C. Y. & CLAGUE, D. 1984. The isotope systematics of a juvenile intra-plate volcano: Pb, Nd and Sr isotope ratios of basalts from Loihi Seamount, Hawaii. *Earth and Planetary Science Letters* **69**, 13–29.

STEIN, M. & HOFMANN, A. W. 1992. Fossil plume head beneath the Arabian lithosphere? *Earth and Planetary Science Letters* **114**, 193–209.

SUN, S. & MCDONOUGH, W. F. 1989. Chemical and isotopic systematics of oceanic basalts: implications for mantle composition and processes. In *Magmatism in the ocean basins* (eds A. D. Saunders and M. J. Norry), pp. 313–45. Geological Society of London, Special Publication no. 42.

WATSON, S. P. & MCKENZIE, D. P. 1991. Melt generation by plumes: a study of Hawaiian volcanism. *Journal of Petrology* **32**, 501–37.

WEAVER, B. L. 1991. Trace element evidence for the origin of ocean-island basalts. *Geology* **19**, 123–6.

WEINSTEIN, Y., NAVON, O. & LANG, B. 1994. Fractionation of Pleistocene alkali basalts from the northern Golan Heights. *Israel Journal of Earth Sciences*, **43**, 63–79.

WHITE, W. M. 1985. Sources of oceanic basalts: radiogenic isotopic evidence. *Geology* **13**, 115–8.

WHITE, R. S. & MCKENZIE, D. P. 1989. Magmatism at rift zones: the generation of volcanic continental margins and flood basalts. *Journal of Geophysical Research* **94**, 7685–730.

WILSON, M. 1993. Geochemical signatures of oceanic and continental basalts: a key to mantle dynamics? *Journal of the Geological Society of London* **150**, 977–90.

WINCHESTER, J. A. & FLOYD, P. A. 1977. Geochemical discrimination of different magma series and their differentiation products using immobile elements. *Chemical Geology* **20**, 325–43.

WITT-EICKSCHEN, G. & KRAMM, U. 1997. Mantle upwelling and metasomatism beneath central Europe: geochemical and isotopic constraints from mantle xenoliths from the Rhon (Germany). *Journal of Petrology* **38**, 479–93.